Studies on Vascular Inflammation and Skeletal Muscle Function Related to Atherosclerotic Diseases

January 2023

Hiroki NAGASE

Studies on Vascular Inflammation and Skeletal Muscle Function Related to

Atherosclerotic Diseases

A Dissertation Submitted to

the Graduate School of Science and Technology,

University of Tsukuba

in Partial Fulfillment of Requirements

for the Degree of Doctor of Philosophy in Science

Doctoral Program in Biology,

Degree Programs in Life and Earth Sciences

Hiroki NAGASE

Table of Contents

Abstract

Atherosclerosis is the pathology which fibro-fatty lesions form in the artery wall, leading to peripheral artery disease (PAD) and several cardiovascular events such as myocardial infarction and stroke, which are of high mortality. Lowering low density lipoprotein (LDL), a particle carrying cholesterol, in the blood have been the major interest for the treatment of atherosclerosis, however growing evidence indicate the significance of inflammation in the artery wall. Regarding PAD, a condition in which major arteries are occluded because of considerably progressed atherosclerosis, while treatment approaches from the vascular side such as lipid lowering and antiplatelets have not been successful, recent studies suggest that exercise training contributes to the treatment of PAD independent of blood flow recovery.

In this study, I firstly examined the involvement of delta-5-desaturase (D5D), a fatty acid metabolizing enzyme that converts dihomo-γ-linolenic acid (DGLA) into arachidonic acid, in an murine model of atherosclerosis to confirm the anti-inflammatory strategy for atherosclerosis treatment and secondly investigated the gene expression alteration caused by exercise in the skeletal muscle of murine PAD models in order to explore the mechanisms that could mimic the benefits of exercise training under PAD conditions.

In chapter 1, compound-326, a D5D-specific inhibitor was administrated to apolipoprotein E knockout (*ApoE* KO) mice with two different protocols for atherosclerosis development. Compound-326 reduced the atherosclerotic lesion area in a dose-dependent manner in both protocols accompanied by decreased blood production of pro-inflammatory arachidonic acid-derived eicosanoids and increased blood production of an anti-inflammatory DGLA-derived eicosanoid. Compound-326 also reduced plasma sICAM-1 levels without altering plasma cholesterol levels in both protocols. These

findings clearly indicate the involvement of D5D and its role in vascular inflammation in atherogenesis.

In chapter 2, normal and diabetic PAD model mice were subjected to exercise training followed by the measurement of mRNA expression in the soleus muscle, RNA sequence analysis and Gene Ontology (GO) analysis to evaluate the acute and chronic effects of exercise in PAD condition. As a result, mRNA expression of skeletal muscle regeneration markers was significantly upregulated in normal PAD mice, and this upregulation was significantly inhibited by exercise training while diabetic PAD mice just showed upward trends of these markers and tended to further upregulate by exercise training. Interestingly, RNA sequence and GO analyses revealed that the types of genes regulated and the directions of the gene expression alteration were different between the two PAD model mice. These results provide significant findings to identify the key molecules or pathways that could mimic the benefits of exercise training under PAD conditions.

In conclusion, the present study provides evidence of significant involvement of D5D in the development of atherosclerosis via inflammatory actions, as well as basic information about exercise-induced transcriptional alterations in the skeletal muscles under PAD conditions. These results contribute to the biology in the fields of vascular inflammation and skeletal muscle function as well as the development of new therapeutic agents and other strategies for the treatment of atherosclerotic diseases.

Abbreviations

15-HETrE	15-hydroxyeicosatrienoic acid
5-LO	5-lipoxygenase
AA	arachidonic acid
ALT	alanine aminotransferase
AMI	acute myocardial infarction
ANOVA	analysis of variance
ApoE	apolipoprotein E
AUC	area under the curve
Col3a1	collagen type III alpha 1 chain
COX-2	cyclooxygenase-2
CVDs	cardiovascular diseases
D5D	delta-5-desaturase
DGLA	dihomo-γ-linolenic acid
ELISA	Enzyme-Linked Immunosorbent Assay
FAL	femoral artery ligation
fMLP	N-Formylmethionyl-leucyl-phenylalanine
GLU	glucose
GO	gene ontology
GPR56	G protein-coupled receptor 56
HPLC	High Performance Liquid Chromatography
IC	intermittent claudication
IC_{50}	50% inhibitory concentration
IL-6	interleukin-6
KO	knockout

LC/MS/MS	liquid chromatography-mass spectrometry
LDL	low-density lipoprotein
LTB$_4$	leukotriene B4
MCP-1	monocyte chemotactic protein-1
Myh3	myosin heavy chain 3
Myf5	Myogenic factor 5
NR4A	nuclear receptor 4A
PAD	peripheral artery disease
PCR	polymerase chain reaction
PDE3	phosphodiesterase 3
PGC1a	proliferator-activated receptor gamma coactivator-1 alpha
PGE$_2$	prostaglandin E2
ROS	reactive oxygen species
Rplp0	ribosomal protein large P0
SD	standard deviation
SEM	standard error of the mean
sICAM-1	soluble intercellular adhesion molecule-1
SREBP-1c	sterol regulatory element-binding protein-1c
TC	total cholesterol
TG	triglycerides
TMM	trimmed mean of the M-value
TXB$_2$	thromboxane B2
UV	ultraviolet

General Introduction

**Pathology and epidemiology of atherosclerosis and PAD**

Cardiovascular diseases (CVDs) are the leading cause of death globally, taking an estimated 17.9 million lives each year in 2019 [1] (Figure 1). The number of deaths is estimated to continue to increase [2] (Figure 2). CVDs are a group of disorders of the heart and blood vessels and include coronary heart disease, cerebrovascular disease, rheumatic heart disease and other conditions. More than four out of five CVD deaths are due to ischemic heart disease and stroke [1].

Leading causes of death globally

○ 2000　● 2019

1. Ischaemic heart disease

2. Stroke

3. Chronic obstructive pulmonary disease

4. Lower respiratory infections

5. Neonatal conditions

6. Trachea, bronchus, lung cancers

7. Alzheimer's disease and other dementias

8. Diarrhoeal diseases

9. Diabetes mellitus

10. Kidney diseases

Number of deaths (in millions)

● Noncommunicable　● Communicable　● Injuries
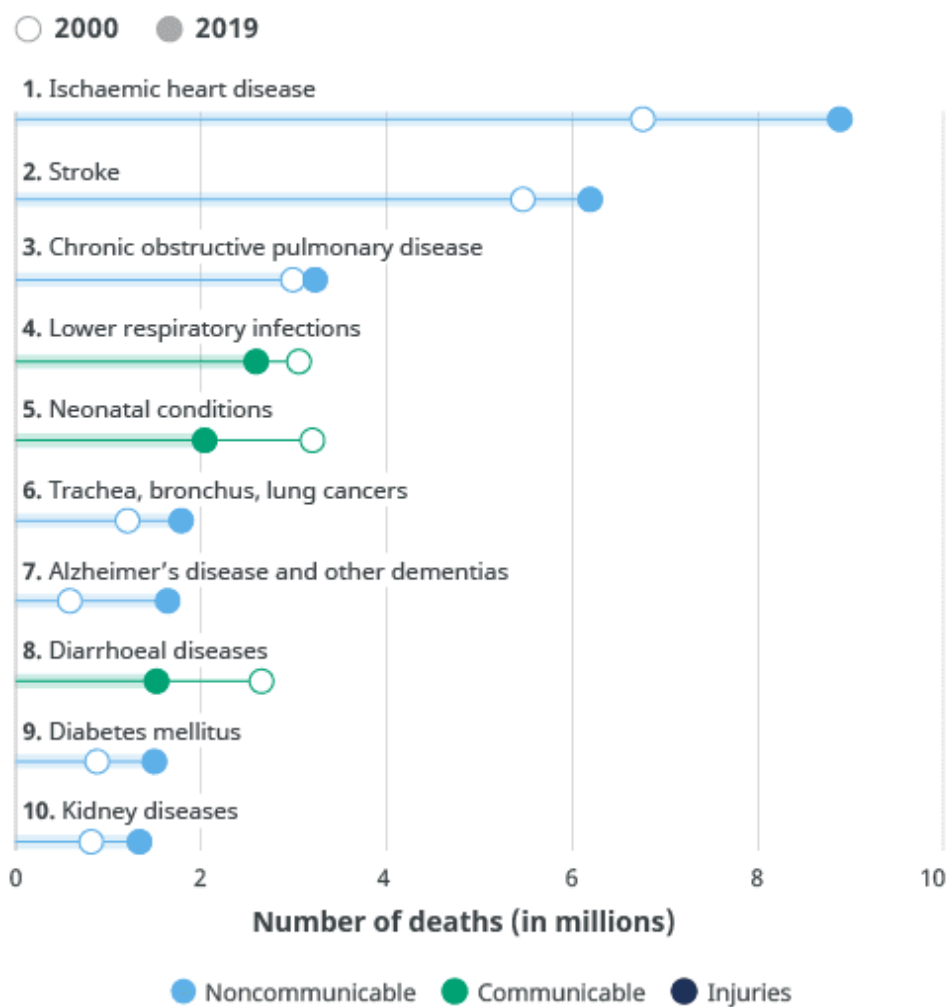
Source: WHO Global Health Estimates.

Figure 1. Leading cause of death globally. Cited from reference [1].

8
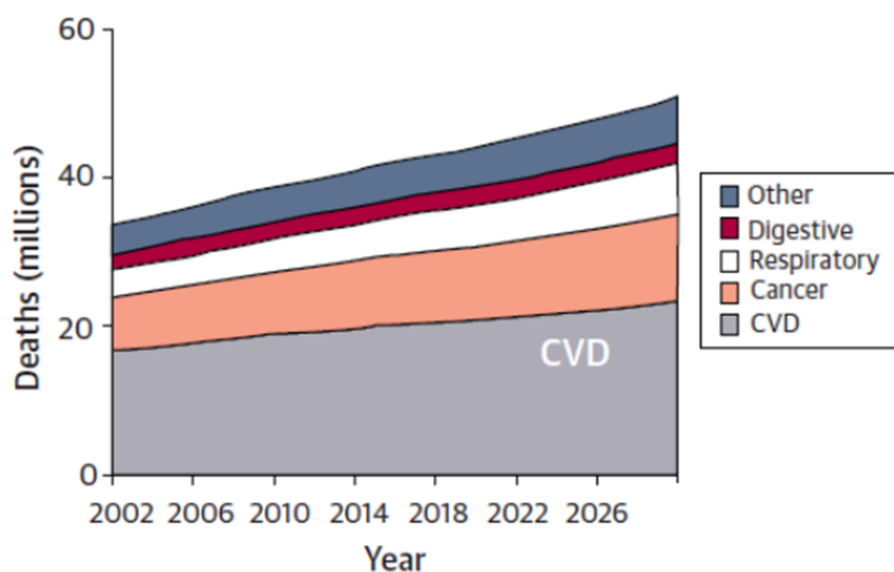
Figure 2. Deaths deriving from chronic diseases. Cited from reference [2].

The pathology that underlies these diseases is atherosclerosis. Thus, novel drugs that can treat atherosclerosis and prevent the subsequent cardiovascular events including ischemic heart disease and stroke are urgently needed in clinical practice [3, 4].

Atherosclerosis is defined as a focal, inflammatory fibro-proliferative response to multiple forms of endothelial injury [5]. While healthy arteries maintain their normal vascular function with no injuries in the intima (Figure 3a), the formation of atherosclerosis starts from the injury in the vascular endothelial cells by risk factors such as hypertension, diabetes, and hyperlipidemia. The damage to the endothelium results in increase of reactive oxygen species (ROS), adhesion molecules and permeability. Consequently, leukocytes and low-density lipoprotein (LDL) infiltrates into the artery wall to form a plaque (Figure 3b). This causes monocyte activation followed by differentiation to macrophages, which takes up oxidized LDL and leads to the formation of foam cells and inflammatory cell recruitment. Excessive growth of foam cells results in rupture of the plaque (Figure 3c) which leads to platelet aggregation and thrombus

9

formation to repair the plaque (Figure 3d). The plaque rupture and repair occur sequentially which allows the thrombus to grow. When the debris from the ruptured plaque clog the coronary or cerebral arteries, they result in ischemic heart disease or stroke, respectively. When the thrombus further grows and eventually occlude the arteries in the lower extremities arteries such as femoral arteries, this will cause peripheral artery disease (PAD) (Figure 3e).
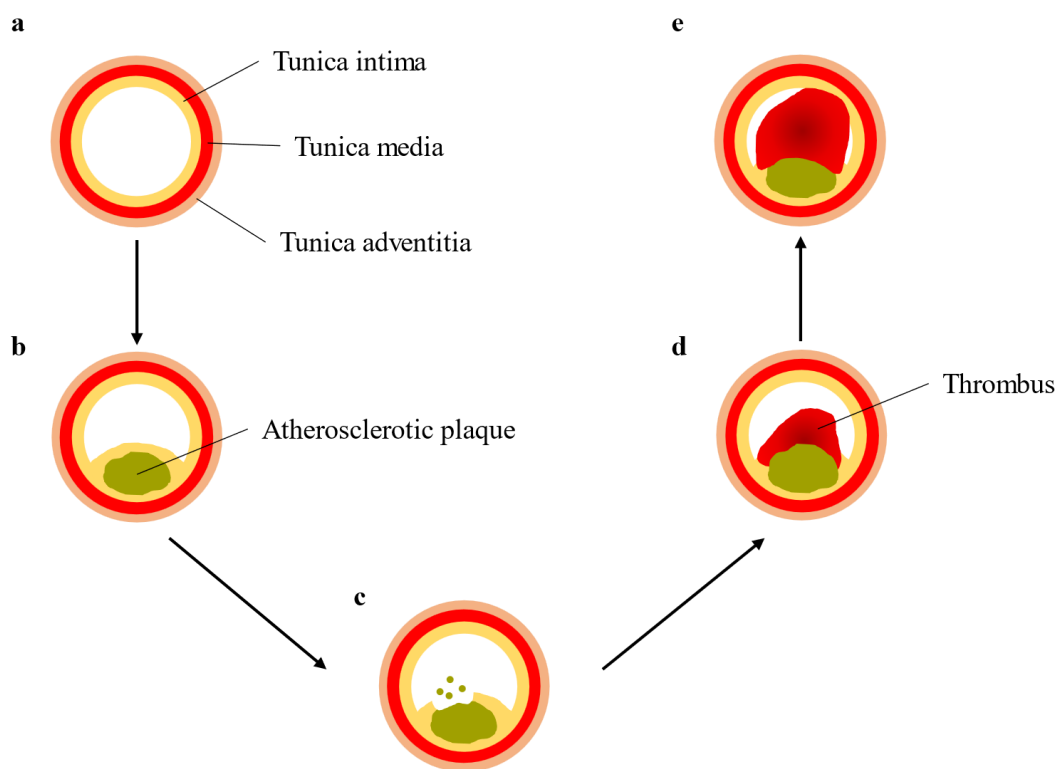
Figure 3. Progressive process of atherosclerosis: Cross-sectional view of an artery. (a) Healthy artery. (b) Atherosclerotic plaque formation caused by leukocytes and LDL infiltration. (c) Plaque rupture caused by excessive growth of foam cells deriving from oxidized LDL uptake by macrophages. (d) Thrombus formation caused by repeated repair and rupture of the plaque. (e) Artery occlusion caused by growth of the thrombus; a pathology observed in PAD patients.

As atherosclerosis progresses throughout the body, the most final form of the pathology is PAD. PAD is characterized by skeletal muscular pain and dysfunction caused by insufficient blood supply [6]. A large population of patients with PAD is affected with concomitant coronary and cerebrovascular diseases, resulting in high mortality and morbidity in developed and developing nations [7]. The most common symptom of PAD is intermittent claudication (IC), characterized by exercise-induced discomfort which is relieved by rest [8]. The primary goal for PAD patients with IC is to improve exercise performance, daily functional activity, and quality of life. Recent evidence revealed that exercise training has beneficial effects in extending the walking distance of PAD patients with IC [9].

Current therapies available for atherosclerosis and PAD

There are several therapies, including pharmaceutical drugs and non-pharmaceutical treatments, acting upon various stages of the pathology of atherosclerosis and PAD.

Lipid lowering agents such as statins are used to prevent initial cholesterol infiltration and the following foam cell formation deriving from oxidized LDL uptake by macrophages [10]. However, even with intense LDL reduction, cardiovascular events, including acute myocardial infarction (AMI), stroke, and cardiovascular death, still occur.

Antiplatelet agents such as $P2Y_{12}$ inhibitors and aspirins are also prescribed to atherosclerosis and PAD patients. These agents prevent excessive thrombus growth associated with plaque rupture [11]. Yet even with sufficient reduction in platelet activity, patients still suffer from critical limb ischemia, a progressed pathology following IC, and even succeeding amputation.

No drug to date has shown significant efficacy against PAD. The only drug that can

improve walking performance in PAD patients with IC to date is cilostazol, a phosphodiesterase 3 (PDE3) inhibitor, however its effect is extremely limited. Recently, endurance exercise training has known to improve the walking performance of PAD patients. A randomized trial of exercise training in addition to optimal medical therapy demonstrated a clear additive benefit even superior to that of aortoiliac revascularization [12]. Exercise training is considered to affect several machineries associated with clinical benefits, including alteration in skeletal muscle metabolism, conditioning underlying diseases, and improving endothelial function [12–15]; however the detailed mechanisms remain unknown. Since exercise training for PAD patients is available in a limited number of facilities and the elderly, who comprise the majority of PAD patients, are often reluctant to perform exercise training, developing drugs that provide the similar benefits is of great social significance. For this purpose, a better understanding of the molecular mechanism underlying the exercise-induced benefits is highly desirable.

Among the progressive process of atherosclerosis illustrated in Figure 3, no drug focuses on the chronic inflammation in the artery wall, one of the most important characteristics of atherosclerosis, to prevent the plaque rupture [5]. Recently, CANTOS trial revealed that canakinumab, an interleukin 1β antibody, showed significantly lower rate of recurrent cardiovascular events independent of plasma lipid lowering [16]. Also, a phase II clinical study of ziltivekimab, an IL-6 receptor antagonist, showed to markedly reduce biomarkers of inflammation and thrombosis in patients with atherosclerosis [17]. These studies suggest that anti-inflammatory strategy for arterial walls could be an effective measure for atherosclerotic plaque stabilization and rupture prevention [18, 19].

Objective of this study

In the present study, I focused on the biology of anti-inflammatory and exercise-induced effects on atherosclerotic diseases which are not fully understood in order to contribute to the discovery of novel treatment strategies.

In chapter 1, in order to gather further preclinical evidence of the involvement of delta-5 desaturase (D5D), an anti-inflammatory-based target, and to confirm its inhibition as a promising strategy in treating atherosclerosis [20, 21], I investigated the efficacy of a specific inhibitor of D5D in murine models of atherosclerosis. Growing evidence including findings from clinical trials show the rationale of the anti-inflammatory strategy for the treatment of atherosclerotic diseases. Because the current therapies available are insufficient, leaving residual risks of cardiovascular events as discussed above, there is still a compelling unmet need for these drugs and therefore significant importance in accumulating data of anti-inflammatory effects on atherosclerosis.

In chapter 2, I explored the gene expression patterns caused by exercise in order to identify key molecules or pathways that could mimic the benefits of exercise training under PAD conditions. Recent studies highlight the involvement of myokines, or bioactive molecules secreted from the skeletal muscles, during exercise. For example, interleukin-6 (IL-6) has hypertrophic effects on skeletal muscles [22–25] and the effects are inhibited by myostatin [26]. Although several reports show the exercise-induced alteration on skeletal muscle gene expression in healthy subjects [27, 28], there are no studies to date in PAD patients or animal models. Because PAD subjects have significant difference in hemodynamic and inflammatory status compared to healthy subjects, it is important to obtain basic gene expression data caused by exercise in PAD conditions.

Chapter 1. Effects of compound-326, a selective delta-5 desaturase inhibitor, in

***ApoE* knockout mice with two different protocols for atherosclerosis development**

Abstract

A previous work on compound-326, a selective delta-5 desaturase (D5D) inhibitor, confirmed its anti-atherosclerotic effects by pre-treatment in Western diet-fed *ApoE* knockout mice. In order to gather further preclinical evidence of the involvement of D5D and to confirm its inhibition as a promising strategy in treating atherosclerosis, effects of compound-326 were evaluated in *ApoE* knockout mice with two different protocols for atherosclerosis development.

In a post-treatment protocol, where the compound treatment started after 10 weeks pre-feeding of Western diet, compound-326 (1 and 3 mg/kg/day, *p.o.* for 12 weeks) significantly reduced the atherosclerotic lesion area in the aorta (24% reduction at 3 mg/kg/day). In another protocol using Paigen diet (containing 12.5% cholesterol and 5% sodium cholate), compound-326 (3 and 10 mg/kg/day, *p.o.* for 7 weeks) also significantly reduced the lesion area (36% reduction at 3 mg/kg/day).

In both protocols, compound-326 significantly reduced the hepatic ratio of arachidonic acid to dihomo-γ-linolenic acid, blood inflammatory eicosanoid production and plasma soluble intercellular adhesion molecule 1 (sICAM-1) levels, similarly to the previous pre-treatment study.

In conclusion, compound-326 exerted anti-atherosclerotic effects in knockout mice with the two different protocols for atherosclerosis development further supporting D5D inhibition as a promising strategy in treating atherosclerosis.

Introduction

Delta-5 desaturase (D5D) is considered an attractive target molecule for treating atherosclerosis [20, 21]. D5D is an enzyme mainly expressed in the liver [29, 30], which metabolizes dihomo-γ-linolenic acid (DGLA) into arachidonic acid [31]. Arachidonic acid is considered to play a role in the progression of atherosclerosis because of its pro-inflammatory properties [32]. Several reports have suggested that D5D gene polymorphism in humans is associated with coronary artery diseases [33, 34]. D5D-deficient apolipoprotein E (*ApoE*) knockout mice were resistant to diet-induced development of atherosclerosis [20, 21]. A recent work discovered that an orally active and selective D5D inhibitor, compound-326, that exhibited *in vitro* D5D inhibition (IC_{50}: 22 nM) in human cells [35], reduced liver and blood arachidonic acid levels in mice, accompanied by an increase in DGLA levels [21]. In *ApoE* knockout mice fed a Western diet for 14 weeks, the atherosclerotic lesion area was significantly reduced by 15-week treatment with compound-326 (1-week pre-treatment plus 14-week concurrent treatment with Western diet). These results suggest that D5D inhibition could be a promising strategy for the treatment of atherosclerosis.

Diet composition and duration are known to affect the characteristics of atherosclerotic plaques [36]. *ApoE* knockout mice fed a Western diet for a long duration showed an atherogenesis process strikingly similar to that seen in humans [37]; Paigen diet (containing high cholesterol and cholate) induced severe dysfunction in the reverse cholesterol transport system [38], resulting in high plasma cholesterol levels and accelerated plaque development in *ApoE* knockout mice. These different diets are known to induce different pathologies and states of inflammation [39, 40]. Since the inflammatory properties of atherosclerosis are known to vary in clinical practice

according to stages of the pathology and to complications in patients [41–44], it is important to evaluate effects of D5D inhibition in several animal models of atherosclerosis with different states of inflammation and different pathophysiology.

In the present study, the anti-atherosclerotic and anti-inflammatory effects of the D5D inhibitor compound-326 were investigated in *ApoE* knockout mice with two different protocols for atherosclerosis development.

Materials and Methods

Animals

Male *ApoE* knockout mice (6 weeks old) were supplied by Takeda Rabics, Ltd (Fukuchiyama, Japan). All animals were maintained on a laboratory chow diet (CE-2, Clea Japan, Suita, Osaka) before experiments. Mice were allowed free access to water and food before and during experiments. The care and use of the animals and the experimental protocols used in this research were approved by the Experimental Animal Care and Use Committee of Takeda Pharmaceutical Co., Ltd., and were in accordance with the Guide to the Care and Use of Experimental Animal Care.

Chemicals

A D5D selective inhibitor, 2-(2,2,3,3,3-pentafluoropropoxy)-3-[4-(2,2,2-trifluoroethoxy)phenyl]-5,7-dihydro-3H-pyrrolo[2,3-d]pyrimidine-4,6-dione, compound-326 (Yashiro et al., 2016), was synthesized. Compound-326 was suspended in 0.5% (w/v) methylcellulose (Wako, Osaka, Japan).

Experimental design for atherosclerosis intervention studies: post-treatment protocol

From 11 weeks of age, mice were fed a Western diet (D12079B, Research Diets, Inc., New Brunswick, NJ, USA) for 10 weeks to develop atherosclerotic lesions. Mice were then divided into four groups (n = 10–14) based on body weight and plasma biochemical parameters (alanine aminotransferase [ALT], total cholesterol [TC], triglycerides [TG], and glucose [GLU]), and 10 mice were dissected to obtain data for this group (Pre group). Compound-326 was administered to the rest of the mice at gravimetric doses of either 1

or 3 mg/kg of body weight per day for 12 weeks. The vehicle group received 0.5% (w/v) methylcellulose without compound-326. Food intake was measured every two weeks. Blood samples for interim measurements of plasma TC and the cell adhesion molecule sICAM-1 were obtained every four weeks from the orbital veins. After 12 weeks of treatment, mice were anesthetized by pentobarbital sodium (50–100 mg/kg, *i.p.*), and blood was collected from the abdominal aorta for eicosanoid analysis and from the caudal vena cava for other analyses. Whole aortas were dissected for quantification of atherosclerotic lesions and livers were dissected for fatty composition analysis and TG content measurement.

Experimental design for atherosclerosis intervention studies: Paigen diet protocol

From 13 weeks of age, mice were fed a control diet (D12337, Research Diets, Inc.) for one week and were divided into five groups (n = 6–12) based on body weight and plasma biochemical parameters (ALT, TC, TG, GLU). Compound-326 was administered at gravimetric doses of either 0.3, 3, or 10 mg/kg of body weight per day for 7 weeks. Control and vehicle groups received 0.5% (w/v) methylcellulose without compound-326. In the latter 4 weeks, the mice were fed a Paigen diet (D12336, Research Diets, Inc., containing 12.5% cholesterol and 5% sodium cholate) except for the control group, which received the control diet throughout the study period. Food intake was measured on week 1, 4, and 6 from the onset of the experiment three days. Blood samples for interim measurements of plasma TC and sICAM-1 were obtained from the orbital veins. After 7 weeks of treatment, mice were anesthetized by pentobarbital sodium (50–100 mg/kg, *i.p.*), and blood was collected from the abdominal aorta for eicosanoid analysis and from the caudal vena cava for other analyses. Whole aortas were dissected for quantification of

atherosclerotic lesions and the livers were dissected for fatty composition analysis and TG content measurement.

Assessment of atherosclerotic lesions

Aortas were carefully cleared of all connective tissues under a dissecting microscope and were cut open, washed with saline, and then fixed in 10% neutral buffered formalin for over 7 days. Aortas were stained with Oil Red O to detect the lipid-accumulated area. The stained areas were analyzed using Image-Pro Plus 6.0 (Media Cybernetics, Rockville, MD, USA) and expressed as a percentage of the surface area of the entire aorta.

Hepatic fatty acid composition analysis

Liver samples were homogenized in 4-fold liver wet weight of saline. The homogenized liver samples were added to a 4.5-fold amount of hexane-isopropanol-butylated hydroxytoluene (60:40:0.01, v/v/w) containing 800 μM margaric acid as an internal standard, and were vortexed for 30 min. The hexane phase was removed to a plastic tube and evaporated to dryness under a nitrogen stream and vacuum. The phospholipid fraction was isolated from the residue using Sep-Pak PSA columns (Waters, Milford, MA, USA), based on previously described procedures [45], and was derivatized using a YMC long- and short-chain fatty acid labeling kit (YMC, Kyoto, Japan). Samples were redissolved in methanol and were analyzed by reverse-phase HPLC using an LC column (6.0φ × 250 mm, Shim-pack XR-ODS, Shimadzu, Kyoto, Japan) and by UV absorbance detection at 230 nm. HPLC solvent conditions were as follows: A mobile phase of acetonitrile-water-trifluoro acetic acid (1,660:340:0.004, v/v/w), a flow rate of 1.4 mL/min, and a temperature of 40°C.

Measurement of hepatic TG contents

Homogenized liver samples were added to an equal amount of 0.4% $CaCl_2$ (w/v) solution and a 4.5-fold amount of hexane-isopropanol-butylated hydroxytoluene (60:40:0.01, v/v/w), and were vortexed for 30 min. The hexane phase was removed to a plastic tube and evaporated to dryness under a nitrogen stream and vacuum. The residues were suspended in nonaethylene glycol monododecyl ether-1,4-dioxane (1:1, v/v). TG contents were determined using a Triglyceride E-test (Wako).

Measurements of plasma ALT, TC, sICAM-1, and MCP-1

Blood samples were centrifuged ($20,000 \times g$) at 4°C for five min to isolate plasma and were 6-fold, 200-fold, and 2-fold diluted with saline for quantification of TC, sICAM-1, and monocyte chemoattractant protein 1 (MCP-1), respectively. ALT and TC levels were determined using a 9000 Series Automatic Analyzer (Hitachi, Tokyo, Japan). sICAM and MCP-1 were assessed by a Mouse Soluble ICAM-1 (CD54) ELISA kit (EMICAM1, Thermo Fisher Scientific, Yokohama, Japan) and a Quantikine Mouse CCL2/JE/MCP-1 kit (MJE00, R&D Systems, Inc., Minneapolis, MN, USA), respectively.

Blood eicosanoid production assay

Blood eicosanoid production assay was performed as described previously [21]. Blood samples were stimulated with 30 μM A23187 and 10 μM fMLP (N-Formylmethionyl-leucyl-phenylalanine), and were incubated at 37°C for 10 min. Samples were centrifuged ($20,000 \times g$) at room temperature for 5 min to isolate plasma. Blood eicosanoid composition was analyzed by LC/MS/MS.

Statistical analysis

Results are expressed as the mean ± SEM. Statistical significance between two groups was determined by Student's t-test (for homogenous data) or Welch's test (for non-homogenous data). Statistical significance between groups of multiple doses of test compounds was determined by a two-tailed Williams' test (for homogenous data) or a two-tailed Shirley-Williams' test (for non-homogenous data). Differences were considered significant at $p < 0.05$.

Results

Post-treatment protocol

Anti-atherosclerotic effects of compound-326

To evaluate the effects of D5D inhibition on atherogenic progression in a post-treatment protocol, atherosclerotic lesions were developed in advance by a 10-week administration of a Western diet to *ApoE* knockout mice (Pre group). The group developed a 14% surface lesion area for the entire aorta, indicating sufficient formation of the atherosclerotic lesion area before the administration of compound-326. The vehicle group developed a 38% atherosclerotic lesion area over additional 12 weeks of the Western diet, indicating continuous atherogenic progression during the drug treatment phase. A 12-week post-treatment with compound-326 (1–3 mg/kg/day, *p.o.*) reduced the atherosclerotic lesion area of the aorta in a dose-dependent manner (16 and 24% reduction at 1 and 3 mg/kg/day, respectively; Figure 4), statistically significant at 3 mg/kg/day. The lesion area reduction was 38% at 3 mg/kg when the Pre group was set as the basal line, so the efficacy of compound-326 was comparable to that seen previously in the previous pre-treatment study [21].

A

B
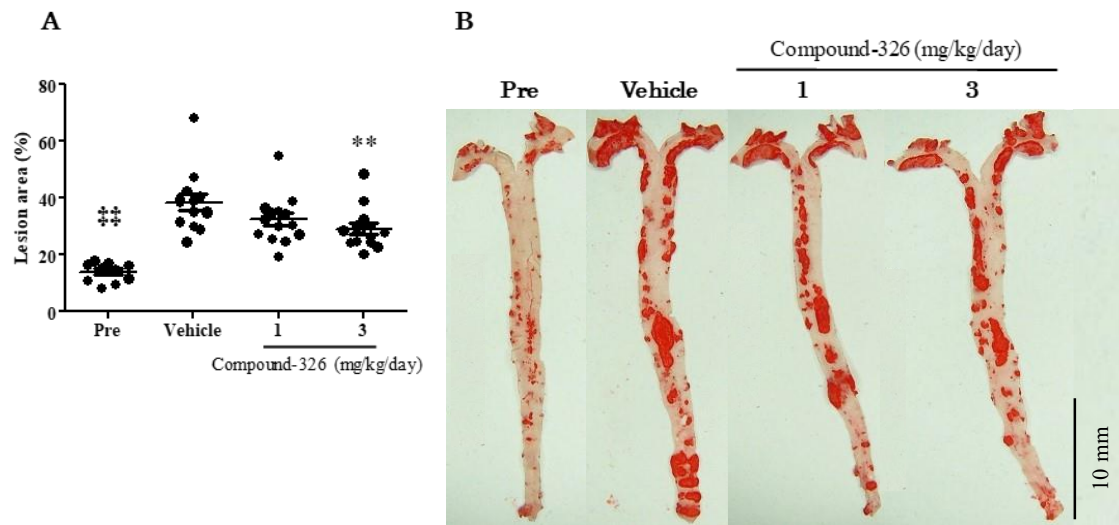
Figure 4. Effects of compound-326 on atherosclerotic lesion area in *ApoE* knockout mice with the post-treatment protocol. Percentage of surface lesion area over the entire aorta were assessed by Oil Red O staining. From 11 weeks of age, mice were fed a Western diet for 10 weeks to develop atherosclerotic lesions. Ten mice were dissected at this point to obtain data for Pre group. Compound-326 was administered to the rest of the mice at gravimetric doses of either 1 or 3 mg/kg of body weight per day. Vehicle group received 0.5% (w/v) MC without compound-326. After 12 weeks of administration, whole aortas were dissected for quantification of atherosclerotic lesions. (A) Percentage of surface lesion area for the entire aorta. (B) Representative images of oil red-O staining of en-face preparations of aortas in each group. Results are expressed as mean ± SEM (Pre: n = 10, others: n = 14). ‡‡$p < 0.01$ vs. vehicle (Welch's test). **$p < 0.01$ vs. vehicle (Williams' test).

In addition, Smirnov-Grubbs' outlier test revealed that the ones with the largest lesion areas in vehicle, 1 mg/kg and 3 mg/kg groups were outliers ($p < 0.05$). When excluded these three outliers, two-tailed Williams' test indicated the statistically significant

reduction of the lesion area in the 1 and 3 mg/kg groups ($p < 0.01$). This analysis suggest that the outliers of the data may affect the statistics.

Effects of compound-326 on fatty acid composition and blood eicosanoid production

To confirm the mechanism of action of compound-326, hepatic fatty acid composition and blood eicosanoid production (stimulated by calcium ionophore A23187 and fMLP) were measured at the end of the treatment period. Compound-326 significantly reduced the reaction product, arachidonic acid contents (33% and 28% reduction at 1 and 3 mg/kg/day, respectively; Figure 5A), and increased the substrate, DGLA contents (163% and 284% increase at 1 and 3 mg/kg/day, respectively; Figure 5B) in the liver in a dose-dependent manner. Compound-326 therefore significantly reduced the arachidonic acid/DGLA ratio in the liver (74% and 81% reduction at 1 and 3 mg/kg/day, respectively; Figure 5C). Similar changes in fatty acid composition were also observed in the blood (data not shown). Corresponding to the composition change in hepatic fatty acids, blood eicosanoid production, a biomarker for D5D inhibitors, was also altered. Arachidonic acid-derived eicosanoids PGE_2 (41% and 43% reduction at 1 and 3 mg/kg/day, respectively; Figure 5D) and TXB_2 (43% and 37% reduction at 1 and 3 mg/kg/day, respectively; Figure 5E) were significantly reduced. Production of LTB_4, an arachidonic acid-derived eicosanoid, in blood was not altered (Figure 5F). A DGLA-derived eicosanoid, 15-HETrE, increased significantly following compound-326 administration (321% and 636% increase at 1 and 3 mg/kg/day, respectively; Figure 5G).
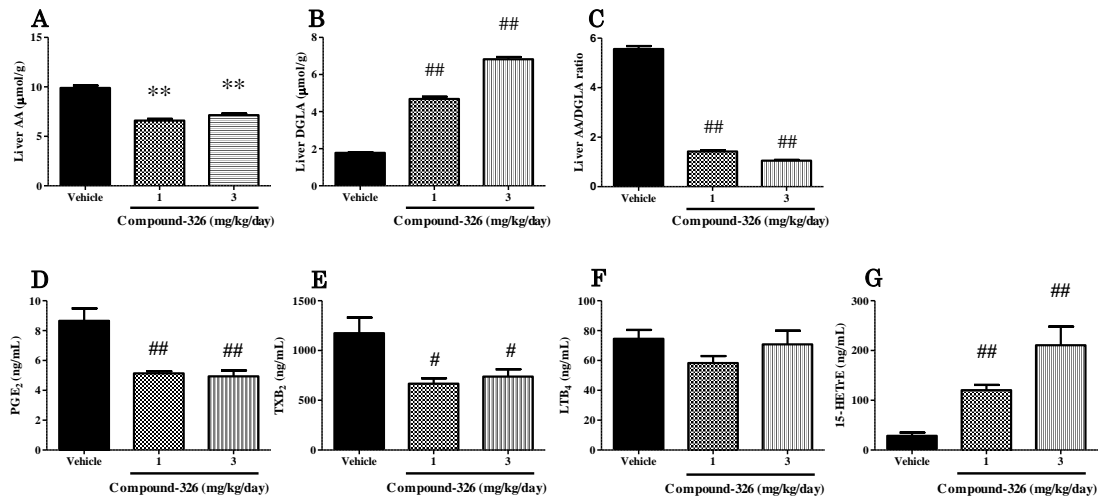
Figure 5. Effects of compound-326 on hepatic fatty acid composition (A-C) and blood eicosanoid production (D-G) in *ApoE* knockout mice with the post-treatment protocol. Livers and bloods were obtained from animals shown in Figure 4 at the end of the study. (A) Arachidonic acid (AA) contents. (B) Dihomo-γ-linolenic acid (DGLA) contents. (C) AA/DGLA ratio. Results are expressed as mean ± SEM (n = 14). (D) PGE_2, an arachidonic acid (AA) derivative. (E) TXB_2, an AA derivative. (F) LTB_4, an AA derivative. (G) 15-HETrE, a dihomo-γ-linolenic acid (DGLA) derivative. Results are expressed as mean ± SEM (n = 7). [**]$p < 0.01$ vs. vehicle (Williams' test). [#]$p < 0.05$, [##]$p < 0.01$ vs. vehicle (Shirley-Williams' test).

Effects of compound-326 on inflammatory markers

Compound-326 suppressed plasma sICAM-1 levels during treatment (Figure 6A), resulting in a significant reduction in area under the curve (AUC) (8.4% reduction at 3 mg/kg/day; Figure 6B). In addition, compound-326 did not alter plasma cholesterol levels (Table 1), suggesting that the anti-atherosclerotic effects were independent of plasma cholesterol levels and were due to anti-inflammatory effects.
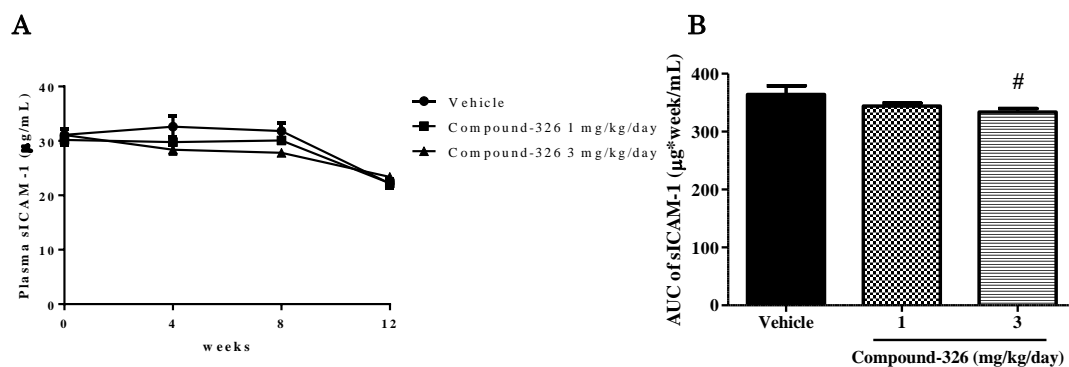
Figure 6. Effects of compound-326 on plasma sICAM-1 levels in *ApoE* knockout mice with the post-treatment protocol. Plasma samples were collected every four weeks from the onset of administration from animals shown in Figure 4. (A) Time-dependent alteration of plasma sICAM-1 levels. (B) Area under the curve (AUC) of plasma sICAM-1 concentrations. Plasma sICAM-1 levels were measured at baseline and on weeks 4, 8, and 12. Results are expressed as mean ± SEM (n = 14). [#]$p < 0.05$ vs. vehicle (Shirley-Williams' test).

Table 1. Effects of compound-326 on plasma total cholesterol (mg/dL) in the post-treatment protocol.

	Weeks after commencing of compound-326 treatment			
Group	**0**	**4**	**8**	**12**
Vehicle	1,459±65	1,451±70	1,349±98	1,313±67
1 mg/kg/day	1,494±55	1,456±59	1,490±51	1,288±56
3 mg/kg/day	1,500±53	1,406±54	1,392±52	1,298±38

Results are expressed as mean ± SEM (n = 14).

Other findings related to compound-326 administration

Compound-326 suppressed Western diet-induced body weight gain (Figure 7). Food intake was not altered (Vehicle: 2.81 ± 0.14 g/day, 1 mg/kg/day: 2.92 ± 0.18 g/day, 3 mg/kg/day: 2.82 ± 0.10 g/day, mean ± SEM, n = 14), indicating that the suppression of body weight gain by compound-326 was independent of food intake.

Liver weight (Vehicle: 1.88 ± 0.14 g, 1 mg/kg/day: 1.87 ± 0.07 g, 3 mg/kg/day: 1.67 ± 0.06 g/day) and hepatic TG (Vehicle: 137 ± 24 µg/mg liver, 1 mg/kg/day: 136 ± 12 µg/mg liver, 3 mg/kg/day: 89 ± 8.3 µg/mg liver) were not altered by compound-326 (mean ± SEM, n=14). Plasma ALT were not altered (Vehicle: 80.3 ± 30.5 U/L, 1 mg/kg/day: 51.0 ± 5.36 U/L, 3 mg/kg/day: 31.3 ± 3.22 U/L, mean ± SEM, n=14) by compound-326.
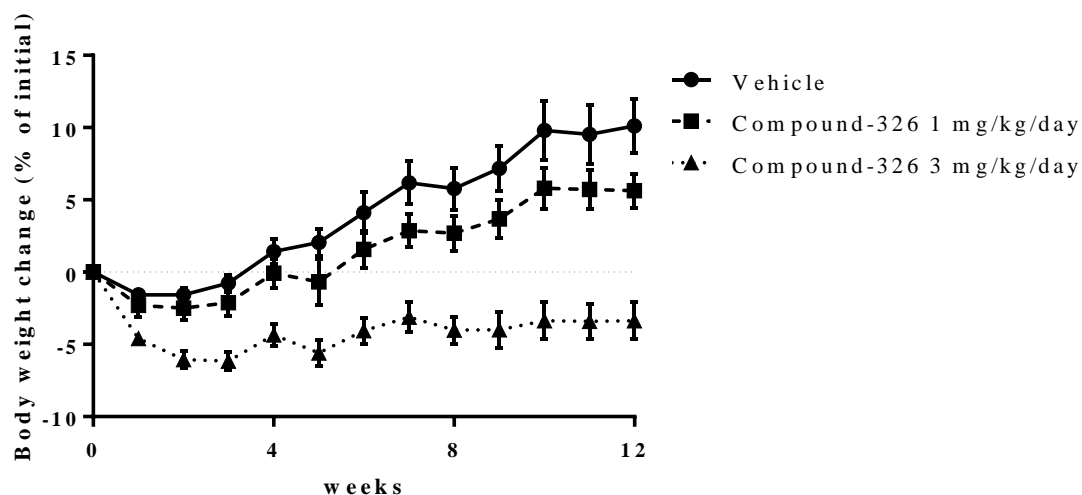

Figure 7. Effects of compound-326 on body weight changes in *ApoE* knockout mice with the post-treatment protocol. Results are expressed as mean ± SEM (n = 14).

Paigen diet protocol

Anti-atherosclerotic effects of compound-326

28

To evaluate the effects of D5D inhibition on atherogenic progression induced by Paigen diet (containing 12.5% cholesterol and 5% sodium cholate), the atherosclerotic lesion area in the aorta was determined after 7 weeks of compound-326 administration (0.3–10 mg/kg/day, *p.o.*, with a 3-week pre-treatment before commencing the Paigen diet). Compound-326 significantly reduced the atherosclerotic lesion area of the aorta in a dose-dependent manner (36% and 38% reduction at 3 and 10 mg/kg/day, respectively; Figure 8).
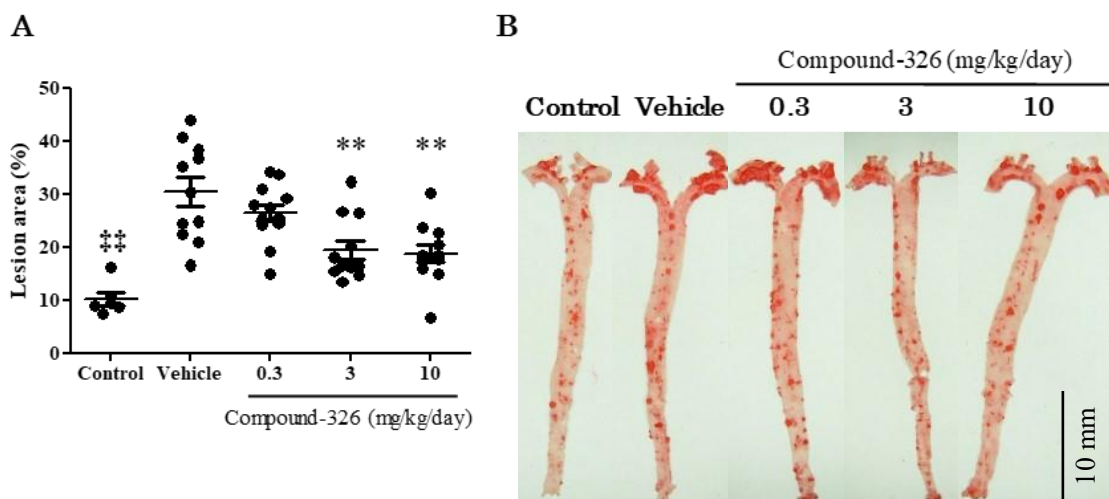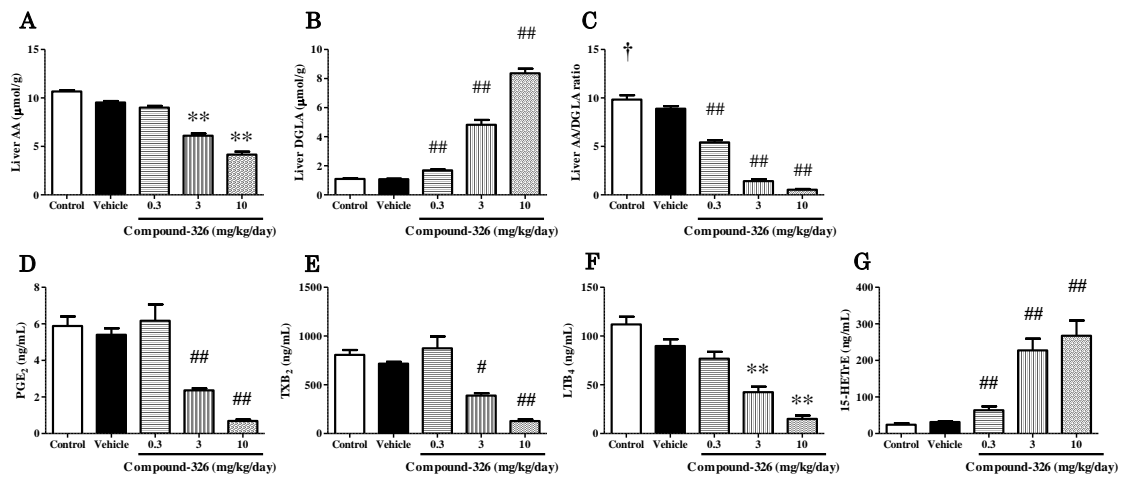

Figure 8. Effects of compound-326 on atherosclerotic lesion area in *ApoE* knockout mice with the Paigen diet protocol. From 13 weeks of age, mice were fed a control diet for one week and were divided into five groups (control: n = 6, others: n = 12). Compound-326 was administered at gravimetric doses of either 0.3, 3, or 10 mg/kg of body weight per day for 7 weeks. Control and vehicle groups received 0.5% (w/v) methylcellulose without compound-326. In the latter 4 weeks, the mice were fed a Paigen diet except for the control group, which received the control diet throughout the study period. After 7 weeks of administration, whole aortas were dissected for quantification of atherosclerotic lesions. (A) Percentage of surface lesion area for the entire aorta. (B)

Representative images of oil red-O staining of en-face preparations of aortas in each group. Results are expressed as mean ± SEM (control: n = 6, others: n = 12). [‡‡]$p < 0.01$ vs. vehicle (Welch's test). [**]$p < 0.01$ vs. vehicle (Williams' test).

Effects of compound-326 on fatty acid composition and blood eicosanoid production

Hepatic fatty acid composition and blood eicosanoid production (stimulated by calcium ionophore A23187 and fMLP) were measured at the end of the treatment period. Compound-326 significantly reduced the product arachidonic acid contents (36% and 56% reduction at 3 and 10 mg/kg/day, respectively; Figure 9A) and increased the substrate DGLA contents (56%, 347%, and 676% increase at 0.3, 3, and 10 mg/kg/day, respectively; Figure 9B) in the liver in a dose-dependent manner. Compound-326 therefore significantly reduced the arachidonic acid/DGLA ratio in the liver (39%, 84%, and 94% reduction at 0.3, 3, and 10 mg/kg/day, respectively; Figure 9C), in a dose-dependent manner. Similar changes in fatty acid composition were also observed in the blood (data not shown). Corresponding to the composition change in hepatic fatty acids, blood eicosanoid production was also altered. Arachidonic acid-derived eicosanoids PGE_2 (56% and 87% reduction at 3 and 10 mg/kg/day, respectively; Figure 9D), TXB_2 (46% and 82% reduction at 3 and 10 mg/kg/day, respectively; Figure 9E), and LTB_4 (53% and 83% reduction at 3 and 10 mg/kg/day, respectively; Figure 9F) were significantly reduced. The DGLA-derived eicosanoid 15-HETrE increased significantly (104%, 626%, and 754% increase at 0.3, 3, and 10 mg/kg/day, respectively; Figure 9G) following compound-326 administration.
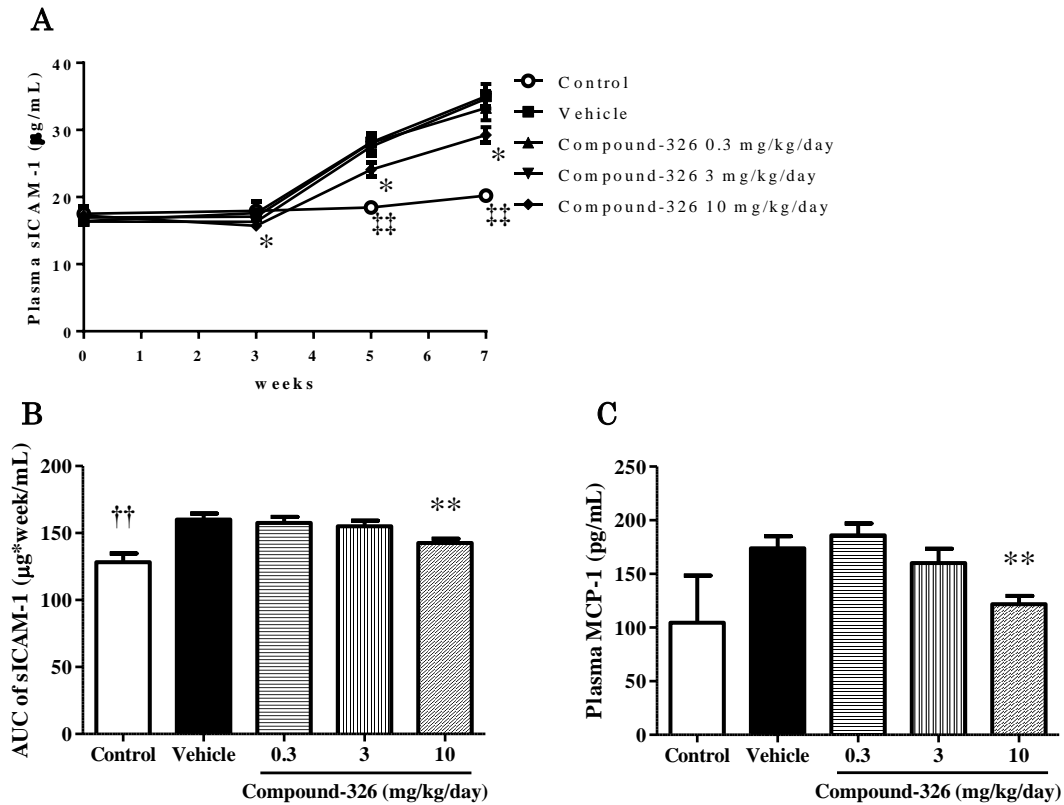
Figure 9. Effects of compound-326 on hepatic fatty acid composition (A-C) and blood eicosanoid production (D-G) in *ApoE* knockout mice with the Paigen diet protocol. Livers and bloods were obtained from animals shown in Figure 8 at the end of the study. (A) arachidonic acid (AA) contents. (B) dihomo-γ-linolenic acid (DGLA) contents. (C) AA/DGLA ratio. Results are expressed as mean ± SEM (control: n = 6, others: n = 12). (D) Prostaglandin E2 (PGE$_2$), an arachidonic acid (AA) derivative. (E) TXB$_2$, an AA derivative. (F) LTB$_4$, an AA derivative. (G) 15-HETrE, a dihomo-γ-linolenic acid (DGLA) derivative. $^{†}p < 0.05$ vs. vehicle (*t*-test). $^{**}p < 0.01$ vs. vehicle (Williams' test). $^{#}p < 0.05$, $^{##}p < 0.01$ vs. vehicle (Shirley-Williams' test).

Effects of compound-326 on inflammatory markers

Compound-326 suppressed plasma sICAM-1 levels during treatment (Figure 10A), resulting in a significant reduction in area under the curve (AUC) (11% reduction at 10 mg/kg/day; Figure 10B). Compound-326 also significantly reduced plasma MCP-1 levels (30% reduction at 10 mg/kg/day; Figure 10C) in a dose-dependent manner. In addition, compound-326 did not alter plasma TC levels (Table 2), suggesting that the anti-atherosclerotic effects were independent of plasma cholesterol levels and were due to

anti-inflammatory effects.

Figure 10. Effects of compound-326 on inflammatory markers in *ApoE* knockout mice with the Paigen diet protocol. Plasma samples were collected on weeks 3, 5, 7 from the onset of administration from animals shown in Figure 8. (A) Time-dependent alteration of plasma sICAM-1 levels. (B) Area under the curve (AUC) of plasma sICAM-1 concentrations. Plasma sICAM-1 levels were measured at baseline and on weeks 3, 5, and 7. (C) Plasma monocyte chemoattractant protein (MCP)-1 concentrations after 7 weeks of treatment. Results are expressed as mean ± SEM (control: n = 6, others: n = 12). ††$p < 0.01$ vs. vehicle (*t*-test). **$p < 0.01$ vs. vehicle (Williams' test).

Table 2. Effects of compound-326 on plasma total cholesterol (mg/dL) in the Paigen diet protocol.

Group	Weeks after commencing of compound-326 treatment			
	0	3	5	7
Control	783±58	803±84	873±88	938±89[††]
Vehicle	787±30	826±34	4,022±131	4,162±112
0.3 mg/kg/day	798±40	820±32	4,275±112	4,219±123
3 mg/kg/day	790±32	856±40	4,297±142	4,260±141
10 mg/kg/day	795±31	801±29	4,271±177	4,084±237

Results are expressed as mean ± SEM (control: n = 6, others: n = 12). [††]$p < 0.01$ vs. vehicle (t-test).

Other findings related to compound-326 administration

Compound-326 enhanced Paigen diet-induced body weight reduction (Figure 11A). Food intake was not altered (Vehicle: 2.88 ± 0.12 g/day, 0.3 mg/kg/day: 2.83 ± 0.13 g/day, 3 mg/kg/day: 2.87 ± 0.11 g/day, 10 mg/kg/day: 2.83 ± 0.14 g/day, mean ± SEM, n = 12), suggesting that the suppression of body weight by compound-326 was not caused by the reduction of food intake. Compound-326 significantly increased liver weight and hepatic TG contents in a dose-dependent manner (Figure 11B, 11C). Plasma ALT were not altered (Vehicle: 75.8 ± 13.3 U/L, 0.3 mg/kg/day: 53.5 ± 6.00 U/L, 3 mg/kg/day: 114 ± 46.1 U/L, 10 mg/kg/day: 54.7 ± 3.88 U/L, mean ± SEM, n = 12) by compound-326.

A

B

C
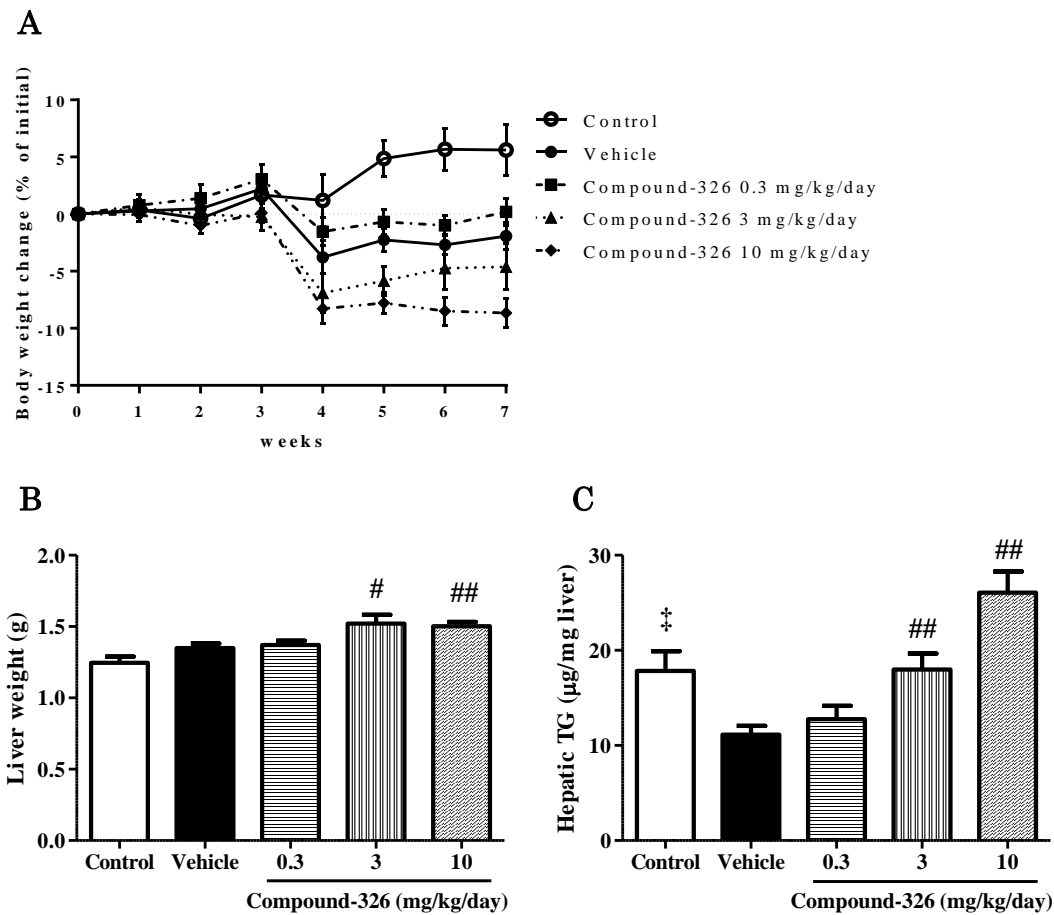
Figure 11. Effects of compound-326 on body weight changes (A), liver weight (B) and hepatic triglyceride (TG) contents (C) in *ApoE* knockout mice with the Paigen diet protocol. (A) Body weight change. Results are expressed as mean ± SEM (control: n = 6, others: n = 12). (B) Liver weight. (C) Hepatic TG contents. Results are expressed as mean ± SEM (control: n = 6, others: n = 12). [‡]$p < 0.05$ vs. vehicle (Welch's test). [#]$p <$ 0.05, [##]$p < 0.01$ vs. vehicle (Shirley-Williams' test).

Discussion

In the present study, I demonstrated that a D5D inhibitor, compound-326, exerts anti-atherosclerotic effects in *ApoE* knockout mice with two different protocols for atherosclerosis development. The main findings in this study were as follows: 1) Compound-326 exhibited anti-atherosclerotic effects in a dose-dependent manner with similar effective dose ranges in the two protocols with different states of inflammation; 2) compound-326 decreased hepatic arachidonic acid levels and increased hepatic DGLA levels in both protocols; 3) compound-326 decreased blood production of arachidonic acid-derived eicosanoids and increased blood production of a DGLA-derived eicosanoid in both protocols; 4) compound-326 reduced plasma sICAM-1 levels without altering plasma cholesterol levels in both protocols; 5) compound-326 exhibited suppressive effects on body weight gain in both protocols; 6) compound-326 increased hepatic TG in *ApoE* knockout mice fed Paigen diet.

This D5D inhibitor exerted anti-atherosclerotic effects in a dose-dependent manner in *ApoE* knockout mice with both protocols. The effective dose ranges in both protocols were similar to those reported in the previous pre-treatment study [21]. In the vehicle-treated groups of this study, Western diet induced a 38.5% atherosclerotic lesion area and a stable sICAM-1 level of approximately 30 μg/mL at 10–22 weeks, while Paigen diet developed a 30.5% atherosclerotic lesion area and a 35 μg/mL sICAM-1 level at 4 weeks. This suggests a clear difference in the relationship between atherosclerotic lesion formation and inflammatory status in these two protocols. Several reports have also indicated that the two diets display different inflammation states. The Paigen diet triggered greater MCP-1 and interleukin-6 (IL-6), gene expression in the mouse aorta compared to that reported with a Western diet. Mice fed the two diets exhibit different

expression patterns of M1 and M2 macrophages, suggesting that the macrophages that accumulate in atherosclerotic lesions vary in polarity. Several other genes are differentially expressed in the two models [37], suggesting a difference in atherogenic progression. Paigen diet-fed mice have been reported not to develop lesions beyond the early foam cells and fatty streaks, while Western diet-fed mice form monocytic adhesions and advanced lesions at earlier stages, displaying a histological similarity to tissues from humans [39]. The Paigen diet itself is inflammatory because of its cholic acid levels, leading to liver toxicity by inducing hepatic NF-κB activation, which is not seen in Western diet-fed mice [39]. These reports outline the differences between the two diet-induced atherosclerosis, supporting the importance of testing drug efficacy in different protocols for atherosclerosis development. It should be pointed out that it is difficult to discuss the impact of the drug efficacy due to the lack of a group for positive control, which is a limitation of this study. Statins, a class of lipid lowering agent widely used for the treatment of atherosclerosis, are ideal positive controls however inappropriate to use in murine studies because mice are statin-resistant. This is because mice have a quite different lipid profile from humans and their compensatory mechanism for lipid lowering is also different from that of humans. One candidate for a positive control could be omega-3 fatty acids, which should be considered in future studies.

D5D inhibition by compound-326 was confirmed in both protocols by a decrease in liver levels of arachidonic acid and an increase in DGLA, a consistent fatty acid compositional alteration in blood, reduced blood production of arachidonic acid-derived inflammatory eicosanoids such as PGE_2, TXB_2, and LTB_4, and increased blood production of DGLA-derived anti-inflammatory eicosanoids such as 15-HETrE. However, the decrease in hepatic arachidonic acid and the reduction in blood production

of arachidonic acid-derived inflammatory eicosanoids did not show a clear dose-dependency in the post-treatment protocol, displaying a maximum effect on arachidonic acid reduction at a dose of 1 mg/kg/day. In contrast, the increase in hepatic DGLA and blood production of DGLA-derived anti-inflammatory eicosanoids showed a clear dose-dependency. Since a 3-mg/kg/day compound-326 treatment showed more potent anti-atherosclerotic effects than the 1-mg/kg/day dose did, these results may suggest the importance of DGLA elevation and DGLA-derived anti-inflammatory eicosanoid increase for D5D inhibition in showing anti-atherosclerotic effects. Several studies have indicated the involvement of eicosanoids in inflammation and atherosclerosis. Studies on mice lacking EP2 and EP4, receptors for PGE_2, described pro-inflammatory and pro-atherogenic properties of PGE_2 [46]. TXA_2 is involved in atherogenesis and ICAM-1 expression in vascular endothelial cells [47]. LTB_4 is reported to promote atherogenesis by inducing MCP-1 production [48, 49]. 15-HETrE has anti-inflammatory properties and has been suggested to exert further anti-inflammatory effects by inhibiting 5-lipoxygenase, an enzyme that converts arachidonic acid into inflammatory eicosanoids [50]. The anti-atherosclerotic effects of DGLA have been previously reported [51], and a DGLA-derived eicosanoid, PGE_1, is thought to be the key to anti-atherosclerotic effects. PGE_1 has been reported to reduce ICAM-1 expression in monocytes, resulting in repression of T-cell infiltration under vascular endothelial cells [52, 53]. Confirming the effects of D5D inhibition on atherosclerotic plaque stabilization should be done in future work by measuring the pathophysiological changes in plaque composition. Taken together, the present results suggest that reduced levels of pro-inflammatory eicosanoids and increased levels of anti-inflammatory eicosanoids exert anti-inflammatory impact, resulting in anti-atherosclerotic effects by D5D inhibition.

In the post-treatment protocol study, treatment of compound-326 did not reduce the LTB$_4$ production despite of the significant reduction in the liver AA content and in the production of PGE$_2$ and TXB$_2$ (Figure 5). This result shows a clear difference from a previous pre-treatment protocol study [21] and the current Paigen diet study (Figure 9), which indicated concurrent decreases in the liver AA content and in the production of PGE$_2$, TXB$_2$ and LTB$_4$. Interestingly, several studies reported that long-term high fat diet feeding enhances the expression of 5-lipoxygenase (5-LO) and 5-LO-activating protein [54, 55]. In the future, it may be interesting to investigate whether the long-term high fat diet feeding may change the balance between LTB$_4$-generating 5-LO pathway and PGE$_2$/TXB$_2$-generating cyclooxygenase-2 (COX-2) pathways in *ApoE* knockout mice, where the 5-LO pathways is known to be activated [56].

Compound-326 reduced plasma sICAM-1 levels without altering plasma cholesterol levels in *ApoE* knockout mice with both protocols, indicating that D5D inhibition can potentially exert anti-inflammatory action. Plasma sICAM-1 levels are a marker of vascular inflammation and a risk factor for cardiovascular diseases [57, 58]. Plasma sICAM-1 levels also can predict future cardiovascular events [59]. One report suggested that high levels of plasma sICAM-1 correlate with a poor prognosis [60]. Regarding the plasma MCP-1 level reduction observed in the Paigen diet protocol, several reports have suggested a relationship between plasma MCP-1 concentrations and atherosclerosis [61, 62]. The anti-inflammatory properties of D5D inhibitors, which are independent of plasma cholesterol levels, can realize further benefits in treating atherosclerosis in addition to statins, the standard treatment [4].

Suppressive effects of D5D inhibition on body weight gain independent of food intake were also confirmed in both protocols in this study, indicating a beneficial and

advantageous aspect of D5D inhibitors. Since D5D inhibition does not alter body weight in normal chow-fed conditions, it is likely that D5D inhibition results in fat mass gain reduction [21]. Several reports refer to the contribution of chronic inflammation to insulin resistance and related metabolic disorders [63, 64]. Previous studies have suggested that D5D inhibition can exert anti-obesity and anti-diabetic effects, accompanied by fat reduction [20, 21, 35]. The study of Yashiro et al. [35] reported that treatment of compound-326 in diet-induced obese C57BL/6J mice decreased expression of macrophage-related inflammatory genes in adipose tissues and increased the whole body energy expenditure, which effects could account for the anti-obesity effects of compound-326. Further analysis should, however, be needed to clarify the underlying mechanisms.

An increase in hepatic TG was observed in the Paigen diet protocol, although it was within the normal range (under 50 μg/mg). Plasma ALT were not concurrently increased, suggesting that the increase in the hepatic TG is a physiological but not a pathological change. My preliminary studies indicate that this hepatic TG increase is observed under specific conditions and depends on diet composition and duration. In fact, the hepatic TG increase was not observed in the present post-treatment protocol. Some studies have suggested that increased lipogenesis related to polyunsaturated fatty acid-mediated regulation of SREBP-1c may be a potential mechanism underlying this phenomenon. Moon et al. (2009) reported that SREBP-1c positively regulated the expression of genes involved in the synthesis of free fatty acid from citrate, and that polyunsaturated fatty acid negatively regulated SREBP-1c expression. Since D5D catalyzes the formation of arachidonic acid, eicosapentaenoic acid, and the downstream product docosahexaenoic acid, which are all polyunsaturated fatty acids [65], inhibiting D5D may attenuate the suppression of SREBP-1c by these polyunsaturated fatty acids, resulting in increased fatty

39

acid and eventual TG synthesis in hepatocytes. This may be a limited effect only in animal experiments since diets used in this study contain poor polyunsaturated fatty acids, unlike clinical situation with exogenous polyunsaturated fatty acid consumption. Future work should elucidate the mechanism underlying this effect, including whether a similar phenomenon occurs in humans.

Chapter 2. Acute and chronic effects of exercise on mRNA expression in the

skeletal muscle of two mouse models of peripheral artery disease

Abstract

Endurance exercise improves walking performance in patients with peripheral artery disease (PAD), which is characterized by skeletal muscle dysfunction caused by lower extremity ischemia. Although transcriptional analyses of exercise-induced changes in normal animals and healthy volunteers have been reported, no detailed study has explored exercise-induced alterations in gene expression in PAD animal models. Here, the acute and chronic effects of exercise on mRNA expression were determined in the skeletal muscles of two mouse models of PAD in order to identify key molecules or pathways that could mimic the benefits of exercise training under PAD conditions. Three particular gene categories were investigated: known exercise-responsive genes (*Pgc1a*, *Il6*, *Nr4a1*, *Nr4a2*, and *Nr4a3*); myogenic and muscle regeneration-related genes (*Myf5, Myogenin, Myomaker*, and *Myh3*); and *Gpr56* and its ligand *Col3a1*. PAD was induced by bilateral femoral artery ligation in normal C57BL/6 and diabetic KK-A^y mice. From 1 week after surgery, repetitive twice-weekly 30-min treadmill endurance exercise sessions were applied. Altered mRNA expression in the soleus muscles was measured in both the acute and chronic phases. In the acute phase, transcript levels of exercise-inducible genes showed significant increases in both C57BL/6 and diabetic KK-A^y PAD mice; levels of regeneration-related genes showed little alteration, and those of *Gpr56* increased immediately and significantly after exercise in both models. In the chronic phase, transcript levels of *Pgc1a*, *Myf5*, *Myogenin*, *Myomaker, Myh3, Gpr56*, and *Col3a1* were upregulated significantly in sedentary C57BL/6 PAD mice compared with that in sham-operated mice. Exercise training inhibited the upregulation of *Col3a1, Myf5*, and *Myogenin* significantly. In KK-A^y PAD mice, only *Gpr56* mRNA levels increased significantly compared with those in sham-operated mice. RNA sequence analysis

revealed 33 and 166 differentially upregulated, and 363 and 99 downregulated, genes after exercise training in C57BL/6 PAD and KK-A^y PAD mice, respectively. In summary, significant alterations were detected from skeletal muscle genes after exercise in PAD mouse models and characterized their expression patterns.

Introduction

Endurance exercise is known to improve walking performance of PAD patients which was proved in a randomized trial of exercise training added to optimal medical therapy, even superior to that of aortoiliac revascularization [12]. Exercise training is considered to affect several machineries associated with clinical benefits, including alteration in skeletal muscle metabolism, conditioning underlying diseases, and improving endothelial function [12–15]; however the detailed mechanisms remain unknown.

There is accumulating evidence that exercise training can induce significant alterations in the expression levels of several genes in skeletal muscles; this effect is considered one of the most important underlying molecular mechanisms of exercise-induced benefits. For instance, interleukin-6 (IL-6), which is locally produced in skeletal muscles in response to exercise [22], is known to increase glucose availability and activate muscle satellite cells, contributing to muscle hypertrophy and regeneration [23, 24, 25]. NR4As (*NR4a1*, *NR4a2*, and *NR4a3*) are other genes that are reported to be induced by endurance exercise in human skeletal muscle [27] and are considered to play a role in exercise-induced benefits through improved muscle energy metabolism [66]. These considerations are largely based on the reported data from experiments on normal animals and healthy volunteers. To the best of my knowledge, to date, no detailed studies have described exercise-induced alterations in gene expression in PAD animal models and patients with PAD.

Bilateral ligation of the femoral arteries (FAL) is one of the most common methods to induce PAD in animal studies. Many investigators [26, 67] have reported that several key characteristics of PAD, including muscle atrophy, apoptosis, fiber type switching, altered myosin heavy-chain expression, and muscle fiber denervation, can be induced in mice

and rats using this surgery. In agreement with the fact that diabetes is an important risk factor for PAD patients [68], diabetic animals such as KK-A^y mice have been reported to show more severe disease phenotypes [69, 70].

Recently, White et al. reported that G protein-coupled receptor 56 (GPR56) might play an important role in muscle hypertrophy associated with resistance/loading-type exercise [71]. A murine model of overload-induced muscle hypertrophy is associated with increased expression of both *Gpr56* and its ligand, collagen type III, whereas genetic ablation of *Gpr56* expression attenuated overload-induced muscle hypertrophy and associated anabolic signaling. In addition, *GPR56* expression was induced in humans by resistance exercise [71]. Although these new findings suggest GPR56 could be an interesting molecular target to mimic the molecular signaling related to exercise-induced clinical benefits, the expression profiles of GPR56 have not been reported in PAD animal models and patients with PAD.

The aim of the present study was to determine the acute and chronic effects of exercise on mRNA expression in the soleus muscles of two mouse models of PAD: normal C57BL/6 mice and diabetic KK-A^y mice with FAL. In particular, three categories of genes were focused: 1) known exercise-responsive genes (*Pgc1a*, *Il6*, *Nr4a1*, *Nr4a2* and *Nr4a3*); 2) myogenic and muscle regeneration-related genes (*Myf5, Myogenin, Myomaker* and *Myh3*); and 3) *Gpr56* and its ligand *Col3a1*. In the present study, whether diabetes could induce exercise-induced transcriptional alterations were also investigated, by comparing the data obtained from the two PAD mouse models.

Materials and Methods

Animals

Male C57BL/6 mice and KK-A^y/Ta mice (8 weeks old) were purchased from CLEA Japan (Tokyo, Japan). All animals were maintained on a laboratory chow diet (CE-2, CLEA Japan) and allowed free access to water and food before and during the experiments. The care and use of the animals and the experimental protocols used in this research were approved by the Institutional Animal Care and Use Committee of Takeda Pharmaceutical Co., Ltd. (Approval code: 00005751)

Bilateral femoral artery ligation (FAL)

C57BL/6 and KK-A^y mice underwent FAL at 12 and 10 weeks of age, respectively. All surgical procedures were performed under isoflurane anesthesia (1–5 %) and buprenorphine analgesia (0.5–1 mg/kg, *s.c.*), and all efforts were made to minimize suffering. After skin incision, the proximal and distal ends of the femoral artery and the proximal profunda femoris artery in the groin were dissected and ligated for both legs. The intervening segments were excised and the dissected sites were sutured with sterile threads. After closing the incision using surgical sutures, the mice were allowed to recover for 7 days. In the sham-operated mice, the same surgical procedure was performed except for the ligation and excision of the artery.

Treadmill exercise training and tissue sampling

Before FAL surgery, all mice were subjected to a 10-min habituation to a treadmill (Panlab) three times, according to the following protocol: 3 m/min for 1 min and 9 m/min for 4 min, on an incline of 5°. Grouping was performed based on body weight for

C57BL/6 mice, and on habituation running time, body weight, and plasma biochemical parameters (glutamic pyruvic transaminase, total cholesterol, triglyceride, glucose, and hemoglobin A1c) for the KK-A^y mice. For exercise training after FAL surgery, mice underwent a total of four to five 30-min treadmill exercise procedures twice a week from 1 week after surgery (exercise groups), according to the following protocol: 3 m/min, 4.2 m/min, 5.4 m/min, 6.6 m/min, and 7.8 m/min for 1 min each; 9 m/min for 5 min; 12 m/min for 10 min; and 15 m/min for 10 min, on an incline of 15°. To monitor the time course of recovery of their running performance, time to exhaustion in each exercise training session was measured. When mice were exhausted, they were allowed to recover (60–90 min), and then returned to the treadmill to achieve a total training time of 30 min. Preliminary experiments revealed that these repetitive twice-weekly treadmill exercise sessions significantly prolonged time to exhaustion on the treadmill test at 3–4 weeks after FAL surgery in both C57BL/6 and diabetic KK-A^y PAD mice. In the sedentary groups, no mice were subjected to the treadmill exercise until the tissue sampling procedure. For acute assessment, mice were euthanized under pentobarbital anesthesia (50–100 mg/kg, *i.p.*) and the right soleus muscles were harvested at the indicated time points (described in the legends of each figure). For chronic assessment, including individual transcript measurement and RNA seq analysis, the soleus muscles were harvested 4 days after the last exercise. In the present study, soleus muscle, which consists predominantly of slow-twitch fibers, were used because preliminary experiments indicated that more genes were significantly altered in the soleus muscle than in the gastrocnemius muscle of these PAD models. The tissues were frozen immediately in liquid nitrogen and stored at −80°C.

Gene expression analysis

Frozen tissues were dissociated using a GentleMACS dissociator (Miltenyi Biotec, Bergisch Gladbach, Germany) in 1 mL of RLT Plus buffer (Qiagen, Hilden, Germany) containing 0.04 M dithiothreitol. After standing at room temperature for 5 min, samples were centrifuged quickly and then 600 μL of each homogenate was digested using QIAshredder (Qiagen) and centrifuged (20 000 × g) for 2 min. The RNA-containing supernatants were purified using an RNeasy Mini kit (Qiagen) and reverse-transcribed using a High-Capacity cDNA Reverse Transcription Kit (Life Technologies, Carlsbad, CA) to obtain cDNA. The mRNA expression levels were then determined by TaqMan quantitative real-time reverse transcription PCR (qRT-PCR; Applied Biosystems, Foster City, CA), using the following predesigned primer/probe sets: *Rplp0*, Mm99999223_gH; *Ppargc1a (Pgc1a)*, Mm01184322_m1; *Il6*, Mm00446190_m1; *Nr4a1*, Mm01300401_m1; *Nr4a2*, Mm00443060_m1; *Nr4a3*, Mm00450074_m1; *Myf5*, Mm00435125_m1; *Myogenin*, Mm00446195_g1; *Tmem8c (Myomaker)*, Mm00481255_m1; *Myh3*, Mm01332463_m1; *Gpr56*, Mm00817704_m1; and *Col3a1*, Mm01254476_m1. Each expression value was normalized to the expression levels of *Rplp0* and calculated relative to the pre-exercise group for the acute phase study and to the sham-operated sedentary group for the chronic phase study.

RNA sequence analysis

Whole mRNA transcript expression analysis was conducted by Macrogen Inc. (Korea). Briefly, cDNA libraries were constructed using the Truseq RNA Sample Preparation kit (Illumina, San Diego, CA) and paired-end RNA sequencing was performed using the Hiseq2000 system (Illumina). RNA-seq data were processed using Array Studio 8.0.0.78

(OmicSoft Corp., Cary, NC) as follows. FASTQ files were mapped using mouse.B38 as the reference library, and then gene annotations were added to the read count values with ensembl.R78. After checking that the mapping rate was over 80%, the read counts of all samples were exported. Statistical analysis was conducted using the R language (https://www.r-project.org/). To calculate Trimmed Mean of the M-value (TMM) for normalization and to identify mRNAs differentially expressed among soleus muscle from diabetic KK-A^y or C57BL/6 mice, a procedure implemented in the edgeR package was applied. The count per million (cpm) was used in the analysis. Before statistical analysis, for genes with a cpm value greater than 1, at least one sample was retained for further analysis. Up- and down- regulated genes were identified as having a p-value less than 0.01 and a fold change greater than 1.5. The BaseSpace Correlation Engine software (formally known as NextBio; https://japan.ussc.informatics.illumina.com/c/nextbio.nb; Illumina, Cupertino, CA) was used to conduct Gene Ontology (GO) analysis.

Measurement of hindlimb blood flow

Mice were kept at 37°C using a BWT-100A animal warming pad (Bioresearch Center, Nagoya, Japan) under isoflurane anesthesia (1–3 %). The heart rate was measured by electrocardiography to maintain consistent anesthesia. The hindlimb blood flow was monitored at 8 and 10 min after the onset of warming, using a MoorLDI2-2λsim laser Doppler imaging system (Moor Instruments, Devon, UK). Mice were then allowed to recover under normal conditions. For each measurement time point, the average blood flow perfusion units were calculated for both hindlimbs, and the average was calculated. The average of both time points was used for analysis. All procedures were performed in a blinded fashion.

Statistical analysis

The results are expressed as the mean $\pm$ SD. Statistical significance between two groups was determined by Student's *t*-test for homogenous data and by Welch's test for non-homogenous data. Statistical significance between groups of multiple time points was determined by a two-tailed Dunnett's test. Two-way ANOVA was performed to evaluate statistical differences in the hindlimb blood flow by FAL surgery and by exercise training. Differences were considered significant if $p < 0.05$.

Results

Characterization of the two PAD mouse models

To characterize the disease phenotypes of normal C57BL/6 and diabetic KK-A^y PAD mice, their hindlimb blood flow was measured by laser Doppler perfusion imaging 3 weeks after FAL surgery (Figure 12A and B). A significant reduction in blood flow was confirmed in both PAD models. KK-A^y PAD mice showed a larger blood flow reduction (60–78 % reduction vs. sham-operated mice) than C57BL/6 PAD mice (33–34 % reduction). In addition, exercise training did not affect the blood flow. It should, however, be noted that the comparison of absolute flow units is a limitation of the study design, because laser Doppler flow assessments cannot be compared accurately mouse to mouse; limited effects of exercise training on the hindlimb blood flow should be confirmed using more suitable methods. Figure 12C shows the recovery time-course of the running performance of exercised C57BL/6 PAD and KK-A^y PAD mice after FAL surgery. KK-A^y PAD mice showed delayed recovery compared with C57BL/6 PAD mice. These results suggest a more severe disease phenotype for diabetic KK-A^y PAD mice than for C57BL/6 PAD mice, which is consistent with other studies [69, 70].
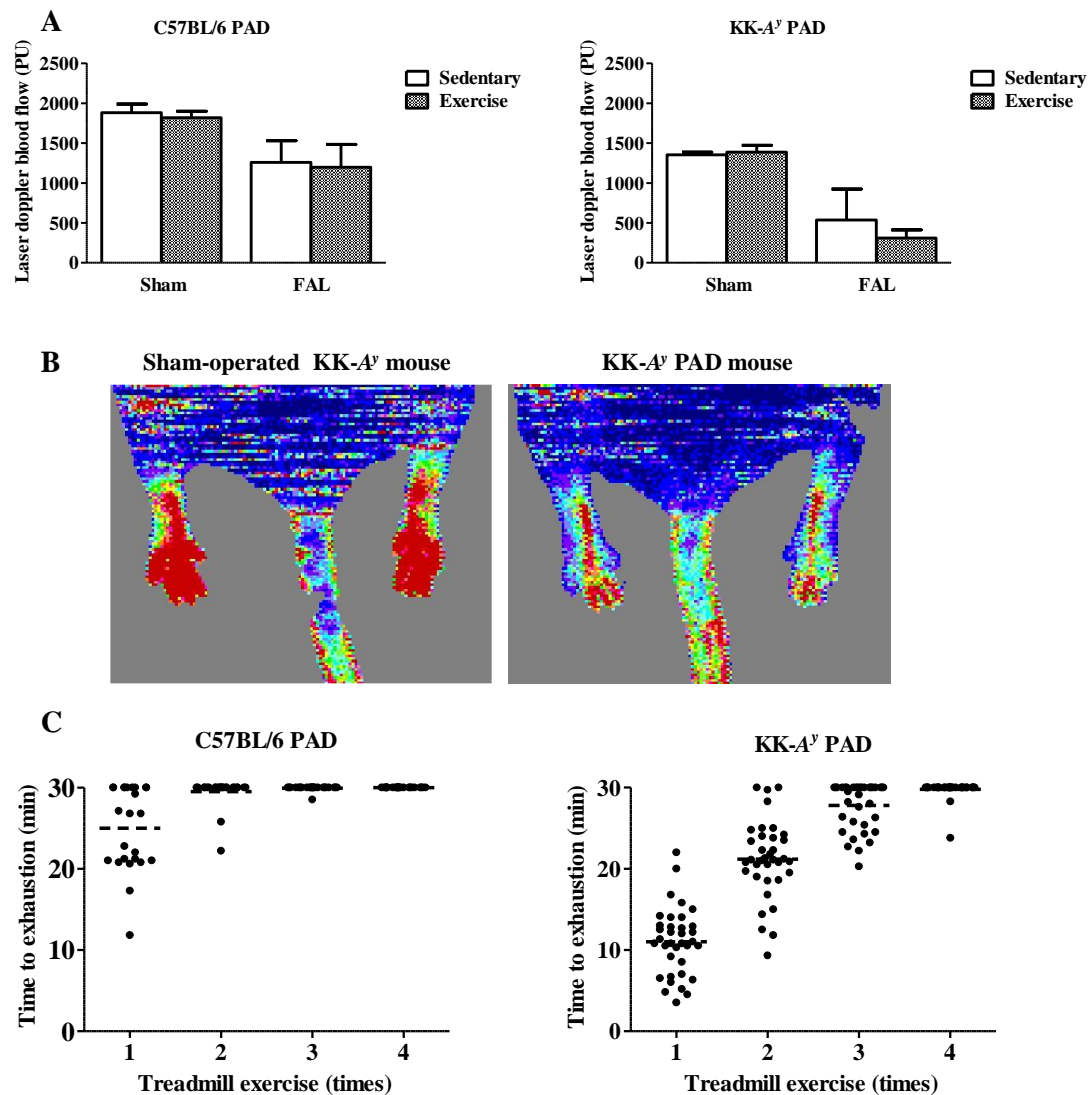
Figure 12. Characterization of the peripheral artery disease (PAD) mouse models.

(A) Hindlimb blood flow in sedentary (open bars) and exercised (closed bars) C57BL/6 PAD (left) and KK-A^y PAD (right) mice 3 weeks after femoral artery ligation (FAL). In the exercise groups, mice were subjected to four 30-min treadmill exercise sessions. In the sedentary groups, no mice were subjected to exercise. Two-way ANOVA revealed significant reductions in blood flow after FAL ($p < 0.01$) in both C57BL/6 PAD and KK-A^y PAD mice. Data are expressed as the mean ± SD, n = 4 for sedentary and exercised sham-operated animals, and n = 8 for sedentary and exercised PAD animals. (B)

Representative laser Doppler perfusion imaging 3 weeks after FAL surgery. Left, sham-operated sedentary KK-A^y mice; right, sedentary KK-A^y PAD mice. In color-coded images, normal perfusion is depicted in red, a marked reduction in blood flow of ischemic hindlimb is in blue. (C) Time course of recovery of the running performance after FAL surgery in exercised C57BL/6 PAD (left) and KK-A^y PAD (right) mice. Dashes represent the mean time to exhaustion for each session in C57BL/6 PAD mice (n = 24) and KK-A^y PAD mice (n = 30).

**Transcripts acutely altered by endurance exercise**

Figure 13 shows the acute alterations of known exercise-responsive genes caused by the endurance exercise protocol in the soleus muscles of both C57BL/6 and KK-A^y PAD mice. The mRNA level of *Pgc1a*, a known exercise-responsive gene, increased significantly and gradually after the exercise session in C57BL/6 PAD (2.1-fold at maximum) and KK-A^y PAD mice (1.7-fold). The mRNA level of another known exercise-responsive gene, *Il6*, also increased significantly immediately after the exercise session in both C57BL/6 PAD (3.4-fold) and KK-A^y PAD mice (5.7-fold). In addition, transcript levels of *Nr4a1*, *Nr4a2*, and *Nr4a3* increased after endurance exercise and then gradually decreased in C57BL/6 PAD mice, peaking at 60–90 minutes after the onset of exercise (2.7, 8.5, and 3.8-fold, respectively; Figure 13C–E). KK-A^y PAD mice also showed upregulation of *Nr4a1*, *Nr4a2*, and *Nr4a3*, with approximately 2-fold greater responses than C57BL/6 mice (7.2, 16, and 6.6-fold, respectively).

Figure 14 indicates the transcript levels of *Myf5*, *Myogenin*, *Myomaker* and *Myh3*, which are known markers of myogenesis and muscle regeneration, in the soleus muscles of both C57BL/6 and KK-A^y PAD mice up to 4 h after the cessation of the exercise. The

mRNA levels of these genes showed little alteration during the observation period.

The mRNA levels of *Gpr56* and its endogenous ligand, *Col3a1*, were determined using the same samples. *Gpr56* transcripts increased immediately and significantly after the exercise session (Figure 15A) in both C57BL/6 PAD (1.9-fold) and KK-A^y PAD mice (1.8-fold). Although the *Col3a1* transcript level showed an increasing trend in both models, the alteration did not reach statistical significance (Figure 15B).
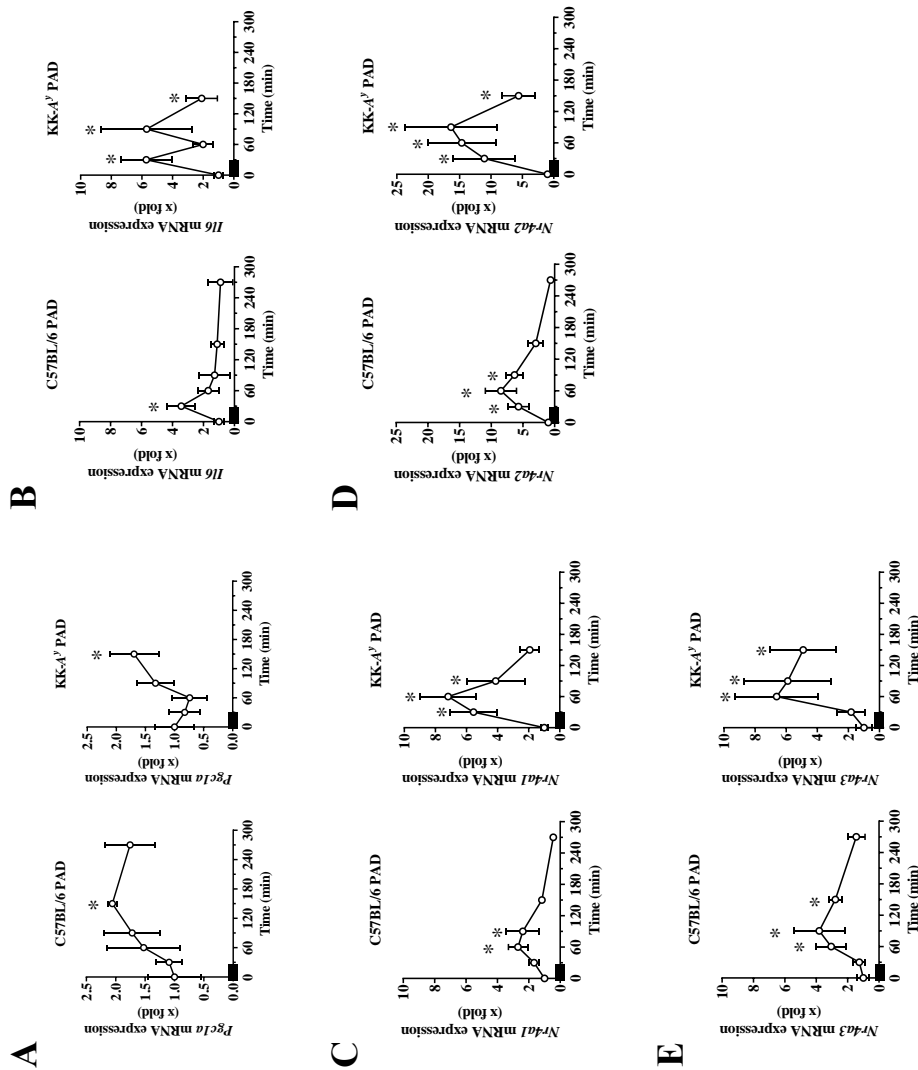
Figure 13. Acute effects of treadmill exercise on the mRNA expression of known

exercise-responsive genes.

The soleus muscles of exercised C57BL/6 PAD mice (n = 4 per time point, total 24, left panels) and KK-A^y PAD mice (n = 6 per time point, total 30, right panels) were obtained before and after the fifth treadmill exercise session. The mRNA expression levels of *Pgc1a* (A), *Il6* (B), *Nr4a1* (C), *Nr4a2* (D), and *Nr4a3* (E) in the soleus muscles were determined by qRT-PCR, normalized to *Rplp0* expression level, and calculated relative to the pre-exercise group (0 min). The results are expressed as the mean ± SD. *$p < 0.05$, **$p < 0.01$ vs. 0 min (Dunnett's test). Bold bars represent the timing of the fifth treadmill exercise.
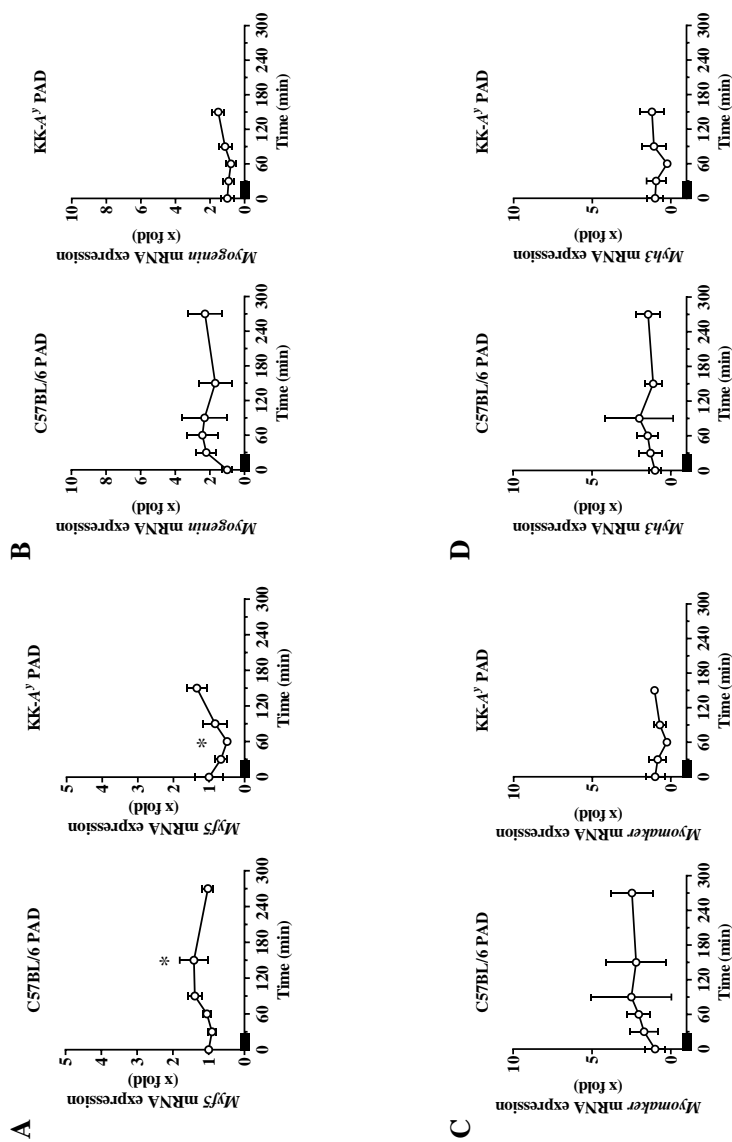
Figure 14. Acute effects of treadmill exercise on the mRNA expression of myogenic and muscle regeneration-related genes

The soleus muscles of exercised C57BL/6 PAD mice (left) and KK-A^y PAD mice (right) were obtained and the mRNA expression levels of *Myf5* (A), *Myogenin* (B), *Myomaker* (C), and *Myh3* (D) in the soleus muscles were determined, normalized, and calculated as described in the legend of Figure 13. The results are expressed as the mean ± SD. Bold bars represent the timing of the fifth treadmill exercise.

56
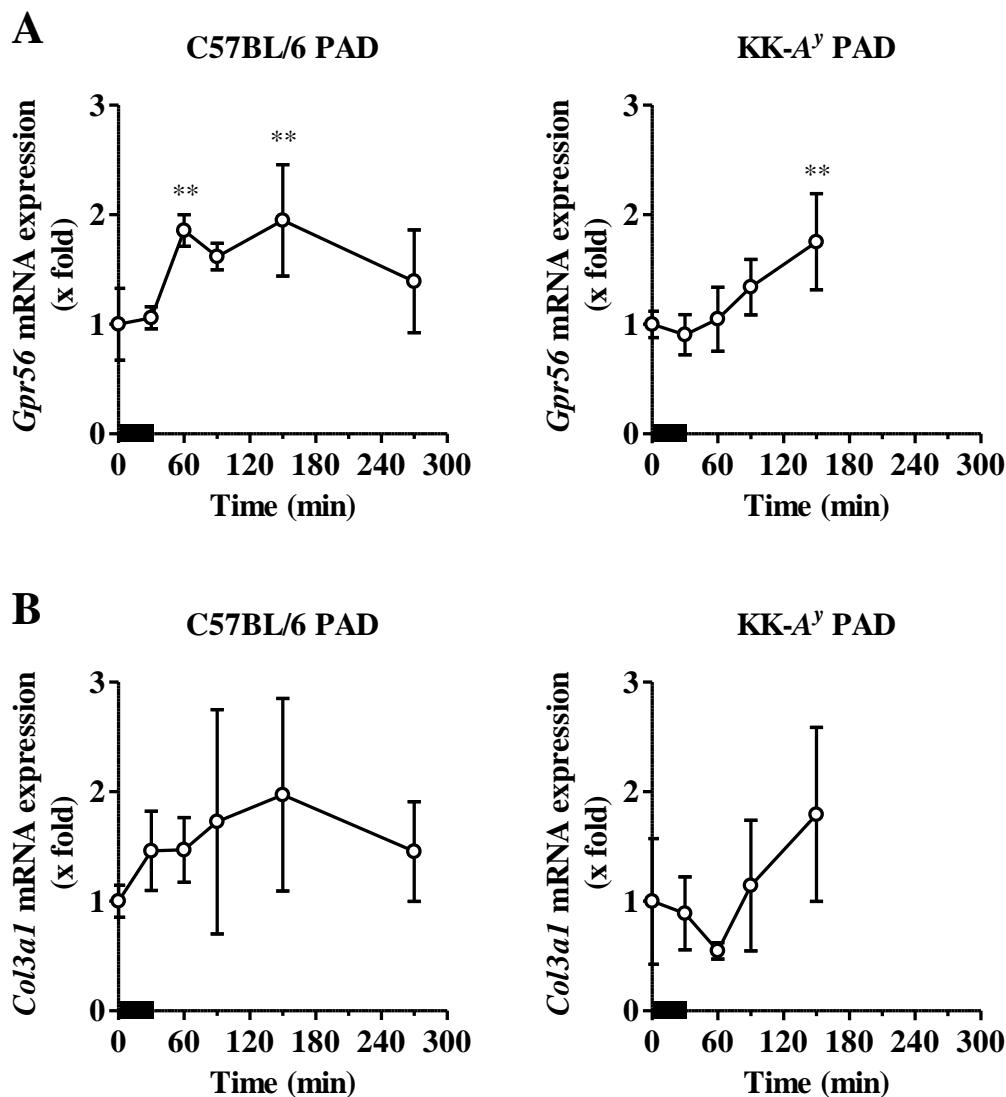
Figure 15. Acute effects of treadmill exercise on the mRNA expression of *Gpr56*

and its ligand, *Col3a1*.

The soleus muscles of exercised C57BL/6 PAD mice (left) and KK-A^y PAD mice (right) were obtained and the mRNA expression levels of *Gpr56* (A) and *Col3a1* (B) in the soleus muscles were determined, normalized, and calculated as described in the legend of Figure 13. The results are expressed as the mean ± SD. **$p < 0.01$ *vs.* 0 min (Dunnett's test). Bold bars represent timing of the fifth treadmill exercise.

Transcripts chronically altered by endurance exercise

Tables 3 and 4 summarize the transcript levels of several genes in the soleus muscles of sham-operated sedentary mice (sham sedentary), sedentary PAD mice (FAL sedentary), and chronically twice-weekly exercised PAD mice (FAL exercise), 3 weeks after FAL surgery.

In C57BL/6 sedentary PAD mice, transcript levels of *Pgc1a*, *Gpr56, Col3a1, Myf5, Myogenin*, *Myomaker*, and *Myh3* were upregulated significantly compared to that in sham-operated mice (Table 3). Exercise training inhibited the upregulation of *Col3a1, Myf5*, and *Myogenin* significantly. No chronic upregulation by exercise was observed in the transcripts of *Il6*, *Nr4a1, Nr4a2*, or *Nr4a*3, which was consistent with the findings of acute and transient induction with rapid recovery after exercise (Figure 13B–E).

Table 3. Chronic effects of treadmill exercise on the mRNA expression in the soleus muscle of C57BL/6 PAD mice.

Gene	Sedentary sham-operated	Sedentary PAD	Exercised PAD
Pgc1a	1.00 ± 0.38	2.87 ± 0.64††	2.26 ± 1.03
Il6	1.00 ± 0.54	1.41 ± 0.35	1.26 ± 0.38
Nr4a1	1.00 ± 0.56	0.66 ± 0.56	0.80 ± 0.11
Nr4a2	1.00 ± 0.37	1.71 ± 0.95	1.61 ± 0.39
Nr4a3	1.00 ± 1.07	1.16 ± 0.21	0.85 ± 0.33
Myf5	1.00 ± 0.15	1.79 ± 0.20††	1.46 ± 0.11‡
Myogenin	1.00 ± 0.35	3.18 ± 0.83††	1.63 ± 0.50‡
Myomaker	1.00 ± 1.08	11.7 ± 5.18††	5.91 ± 3.86
Myh3	1.00 ± 0.42	12.7 ± 3.26††	10.9 ± 4.24
Gpr56	1.00 ± 0.22	1.77 ± 0.50†	1.22 ± 0.40
Col3a1	1.00 ± 0.02	11.0 ± 1.78††	6.70 ± 0.98‡‡

Results are expressed as the mean ± SD; sedentary sham-operated mice (n = 3), sedentary PAD mice (n = 5), and exercised PAD mice (n = 4)

[†]$p < 0.05$, [††]$p < 0.01$ *vs*. sedentary sham-operated mice (Student's or Welch's *t*-test).

[‡]$p < 0.05$, [‡‡]$p < 0.01$ *vs*. sedentary PAD mice (Student's or Welch's *t*-test).

In KK-A^y PAD mice, no significant upregulation was observed in *Myf5*, *Myogenin*, or *Myomaker* mRNA levels compared with those in sham-operated mice, whereas the *Gpr56* and *Myh3* mRNA levels increased significantly (Table 4). Exercise training exerted little effect on the mRNA levels of the genes investigated; only *Myf5* mRNA was upregulated

59

significantly by exercise in KK-A^y PAD mice (Table 4).

Table 4. Chronic effects of treadmill exercise on mRNA expression in the soleus muscle of KK-A^y PAD mice.

Gene	Sedentary sham-operated	Sedentary PAD	Exercised PAD
Pgc1a	1.00 ± 0.30	3.30 ± 1.96	2.21 ± 0.74
Il6	1.00 ± 0.25	2.27 ± 1.38	1.55 ± 0.48
Nr4a1	1.00 ± 0.60	1.29 ± 0.26	1.01 ± 0.23
Nr4a2	1.00 ± 0.16	3.74 ± 2.76	2.90 ± 0.97
Nr4a3	1.00 ± 0.46	5.92 ± 4.13	4.09 ± 2.05
Myf5	1.00 ± 0.09	1.20 ± 0.38	2.31 ± 0.89‡
Myogenin	1.00 ± 0.10	2.20 ± 0.84	3.35 ± 1.24
Myomaker	1.00 ± 1.23	4.38 ± 5.23	9.81 ± 5.99
Myh3	1.00 ± 0.49	4.62 ± 2.08†	8.80 ± 4.40
Gpr56	1.00 ± 0.17	2.09 ± 0.56†	1.74 ± 0.21
Col3a1	1.00 ± 0.20	11.1 ± 9.44	9.74 ± 5.58

Results are expressed as the mean ± SD; sedentary sham-operated mice (n = 4), sedentary PAD mice (n = 4), and exercised PAD mice (n = 6).

†$p < 0.05$ *vs*. sedentary sham-operated mice (Student's or Welch's *t*-test).

‡$p < 0.05$ *vs*. sedentary PAD mice (Student's or Welch's *t*-test).

To identify differentially expressed genes between sedentary and exercised PAD mice, RNA sequence analysis was also conducted using the same sedentary and exercised PAD

mouse samples (Tables 5–8). RNA sequence analysis revealed 33 upregulated and 363 downregulated genes in the soleus muscles of exercised C57BL/6 PAD mice (Tables 5 and 6). In KK-A^y PAD mice, 166 genes were upregulated and 99 genes were downregulated by the exercise training (Tables 7 and 8). Among these differentially expressed genes, only 37 genes overlapped between C57BL/6 PAD mice and KK-A^y PAD mice. Moreover, most (31 of 37) of these overlapped genes were downregulated in C57BL/6 PAD mice, but upregulated in KK-A^y PAD mice, showing a negative correlation.

Table 5. List of differentially upregulated genes in the soleus muscle of exercised C57BL/6 PAD mice.

Gene Symbol	FC	Gene Symbol	FC	Gene Symbol	FC
Irs2	2.68	*Kcnj2*	1.66	*Vgll2*	1.59
Hsbp1l1	2.19	*Slc25a33*	1.66	*Rcan1*	1.57
Otud1	1.80	*Acot2*	1.65	*Ptpn3*	1.56
4632428C04Rik	1.79	*Rbp7*	1.65	*Mlycd*	1.56
Abra	1.79	*Fam134b*	1.64	*Mreg*	1.55
Slc25a34	1.79	*Ier3*	1.64	*Ramp1*	1.54
Nuak1	1.74	*Klf15*	1.63	*Thrb*	1.53
Zbtb10	1.73	*6230400D17Rik*	1.62	*Pde4d*	1.53
Sh3rf2	1.71	*Klhl34*	1.61	*Nfil3*	1.53
C1qtnf4	1.70	*Klf4*	1.61	*Lmod2*	1.51
Hspa1a	1.68	*Nr4a1*	1.59	*Dnajb5*	1.50

FC, fold change.

Sedentary PAD mice (n = 4) and exercised PAD mice (n = 4). Differentially upregulated genes met an average FC criterion of >1.5.

Table 6. List of differentially downregulated genes in the soleus muscle of exercised C57BL/6 PAD mice.

Gene Symbol	FC	Gene Symbol	FC	Gene Symbol	FC
Chga	-41.09	*Ror2*	-2.80	*Gdf11*	-1.97
Wnt16	-29.94	*Fam83g*	-2.79	*Sulf1*	-1.97
Dlk1	-26.98	*Cd109*	-2.79	*Adcy7*	-1.96
Tnn	-24.17	*Cpxm1*	-2.78	*2610203C20Rik*	-1.96
Rspo2	-23.43	*Sntb1*	-2.77	*Has2*	-1.95
Prr32	-16.48	*Prc1*	-2.76	*Sytl2*	-1.95
Rtl1	-15.48	*Enpp1*	-2.74	*Vgll3*	-1.94
Lgr5	-15.05	*Col6a3*	-2.73	*Scd2*	-1.93
Arhgap36	-14.34	*Slc37a2*	-2.67	*Il1rl2*	-1.93
Krt8	-14.31	*Rbp4*	-2.67	*BC023105*	-1.93
Mmp12	-12.99	*Avpr1a*	-2.67	*Pthlh*	-1.92
Dcx	-12.88	*Csrp2*	-2.67	*Fam114a1*	-1.92
Cldn2	-12.21	*Ccl21a*	-2.66	*Rbp1*	-1.91
Krt18	-11.56	*Dkk3*	-2.62	*Klhl13*	-1.91
Lrrc15	-11.08	*Pcdhgb1*	-2.62	*Myo5a*	-1.91
Mest	-10.79	*Peg3*	-2.61	*Arnt2*	-1.91
C1qtnf3	-10.05	*Ephb3*	-2.60	*Itga11*	-1.90

Nrk	-10.04	Adamts20	-2.60	Mfap5	-1.90
Mirg	-9.65	Rnasel	-2.60	Frzb	-1.90
Rian	-9.25	Il20rb	-2.59	Rab31	-1.90
Meg3	-8.99	Basp1	-2.59	Col24a1	-1.90
Dsp	-8.96	Mfsd7a	-2.58	Rbms3	-1.90
Ptn	-8.85	Gldn	-2.58	Cdkn1a	-1.89
Ripply1	-8.82	E2f1	-2.56	Tfpi	-1.89
AW551984	-7.95	Cercam	-2.54	Bex1	-1.89
Myh4	-7.67	Tnfrsf11a	-2.54	Sorbs2	-1.86
Actc1	-7.54	Gamt	-2.53	Mtcp1	-1.86
Tro	-7.47	Ptprf	-2.53	Igtp	-1.85
Myl4	-7.16	Mdga1	-2.52	Mrc1	-1.85
Peg10	-7.01	Itga9	-2.51	Boc	-1.84
Atp6v0d2	-6.96	Thbs2	-2.50	Mir99ahg	-1.84
Fbn2	-6.82	Prkag3	-2.50	Npas2	-1.84
Postn	-6.60	Nr5a2	-2.47	Sfn	-1.84
Slc6a19	-6.55	Ccdc141	-2.47	Serf1	-1.84
Th	-6.51	Efs	-2.45	Gbp5	-1.84
Msln	-6.23	Kcnc4	-2.45	Gpc3	-1.84
Mybph	-6.21	Tdrd9	-2.43	Olfr558	-1.83
Spon1	-5.74	Bid	-2.42	Arhgap22	-1.83
Myh3	-5.67	Serpinb6b	-2.41	Dlg4	-1.83
Slfn4	-5.34	Vcan	-2.40	Lepre1	-1.82

Aldh3a1	-5.25	Adamts7	-2.40	Arhgap32	-1.81
Plagl1	-5.09	Fndc1	-2.39	Sh3tc1	-1.81
Fjx1	-4.99	Srpx2	-2.37	Armcx6	-1.80
Klf14	-4.92	Igf1	-2.37	Selp	-1.80
Cthrc1	-4.89	Atp1b2	-2.36	Plat	-1.80
Gdnf	-4.83	Gatm	-2.36	Dupd1	-1.80
Grem2	-4.78	Eda2r	-2.36	Tnfaip3	-1.79
Glipr1	-4.64	Usp18	-2.36	Klhdc8b	-1.78
Gpr65	-4.59	Tubb6	-2.35	Bicc1	-1.78
Zfp365	-4.38	Ddah1	-2.35	Rap2b	-1.77
Tnnt2	-4.34	Orai2	-2.34	Irf8	-1.77
6330403K07Rik	-4.33	Pi15	-2.33	Klf10	-1.77
Sprn	-4.26	Tnfrsf23	-2.33	Mustn1	-1.76
Adamts16	-4.26	Emilin1	-2.33	Vav3	-1.76
Igfn1	-4.22	Chst2	-2.33	Birc3	-1.76
Lair1	-4.22	Itga4	-2.32	9430073C21Rik	-1.76
Tnc	-4.19	Nhs	-2.32	Nabp1	-1.75
Cemip	-4.06	Fbln7	-2.30	Morc4	-1.75
Begain	-3.97	Kcnq1ot1	-2.30	Rcn1	-1.75
Ddc	-3.95	Fam109b	-2.30	Sh3bp1	-1.75
Pmp2	-3.90	Parm1	-2.29	Zfp948	-1.75
A930003A15Rik	-3.89	Anxa8	-2.28	Ttyh2	-1.74
Scn5a	-3.88	Lhfpl2	-2.28	Zc2hc1a	-1.74

Oasl1	-3.87	Rtp4	-2.27	4933439C10Rik	-1.74
Prnd	-3.81	Sulf2	-2.26	Gpx7	-1.73
Col12a1	-3.76	Ccbe1	-2.26	Efemp2	-1.72
Kcnk1	-3.74	Lyve1	-2.26	Fkbp14	-1.72
Slfn8	-3.71	Adamts3	-2.25	Pycr1	-1.71
Fam65c	-3.69	Ogn	-2.24	G0s2	-1.71
Mss51	-3.68	Osr2	-2.24	Rsad2	-1.71
Ankrd1	-3.64	Lsp1	-2.24	Stk17b	-1.71
Ifit3	-3.54	Primpol	-2.22	Junb	-1.70
Xlr3b	-3.53	Vash2	-2.22	Malat1	-1.70
Dnm3os	-3.51	Traf4	-2.21	Htra1	-1.69
Map3k7cl	-3.50	Fat1	-2.21	Camk2d	-1.69
Ifit1	-3.45	A930004D18Rik	-2.21	Mob3c	-1.69
Apol9b	-3.42	Igsf3	-2.20	Sdc2	-1.68
Fibin	-3.42	Mndal	-2.20	Man1a	-1.68
Nov	-3.41	Msc	-2.17	Igsf1	-1.68
Tceal7	-3.39	Ankrd35	-2.17	Angptl2	-1.66
Piezo2	-3.37	Igfbp4	-2.16	Col5a3	-1.66
Zim1	-3.36	Trp63	-2.16	Atp10a	-1.66
Ccna2	-3.33	Plekha7	-2.16	Rin2	-1.66
Cpne2	-3.31	Gpr64	-2.16	Numbl	-1.66
Lox	-3.31	Rgs10	-2.15	Daam2	-1.65
Fcgr1	-3.30	Elovl6	-2.14	Tnfsf10	-1.65

Dclk1	-3.30	Rcor2	-2.14	Chst12	-1.65
Cx3cr1	-3.29	Tnfrsf22	-2.14	Nes	-1.65
Pvalb	-3.27	Ckap4	-2.14	Dab2	-1.64
Pamr1	-3.19	Fap	-2.14	Ext1	-1.63
Actn3	-3.17	Matn2	-2.12	Mdm4	-1.63
Gadd45a	-3.16	Cd44	-2.12	Kdelc2	-1.62
Plod2	-3.12	Pdk3	-2.11	Chpf2	-1.62
Rec8	-3.10	Mrc2	-2.10	Tspan9	-1.62
Capn6	-3.09	Galnt16	-2.10	Ccdc102a	-1.62
Aspn	-3.08	Mybpc2	-2.10	Scai	-1.61
Zap70	-3.07	Tas1r1	-2.10	AI480526	-1.60
Hmcn1	-3.06	Cdr2l	-2.09	Sesn2	-1.59
I830012O16Rik	-3.06	Entpd7	-2.09	Gprc5c	-1.59
Oasl2	-3.02	Slc25a24	-2.08	Fam65b	-1.59
Oas1a	-3.01	Zfp760	-2.08	Fndc3b	-1.59
Col5a2	-3.00	Tmsb10	-2.07	Atp13a3	-1.59
Ptch2	-3.00	Sertad4	-2.07	Zfp503	-1.57
Col7a1	-2.97	Abi3bp	-2.06	C130074G19Rik	-1.56
Alx4	-2.96	Ifi203	-2.06	Aebp1	-1.56
Myog	-2.96	Fbxl22	-2.06	Tanc2	-1.56
Lrrc55	-2.96	Loxl1	-2.04	Sort1	-1.56
C1ql3	-2.96	Myod1	-2.04	Ift122	-1.55
Sfrp2	-2.95	Spred3	-2.04	Ppp1r3d	-1.55

Mex3a	-2.93	*Dse*	-2.03	*Fmr1*	-1.55
Cacnb3	-2.92	*S100a4*	-2.02	*Iffo1*	-1.55
Mmp3	-2.92	*Cdkn1c*	-2.01	*Ctsz*	-1.54
Ryr3	-2.92	*Lgals3bp*	-2.01	*Pear1*	-1.52
Mstn	-2.91	*Atp1b4*	-2.01	*Ttc14*	-1.52
Mmp23	-2.90	*Zfp354c*	-2.00	*Mid1*	-1.52
Gxylt2	-2.90	*Mafa*	-2.00	*Tmem44*	-1.52
Wisp1	-2.89	*Adam19*	-2.00	*Mtap*	-1.52
Marcksl1	-2.88	*Gk5*	-2.00	*Lgals1*	-1.52
Trim46	-2.87	*Bbc3*	-1.99	*Txndc5*	-1.51
D430019H16Rik	-2.85	*Hps1*	-1.98	*Dusp6*	-1.51
Foxd3	-2.82	*Pcdh18*	-1.97	*Creb3l2*	-1.50

FC, fold change.

Sedentary PAD mice (n = 4) and exercised PAD mice (n = 4). Differentially downregulated genes met an average FC criterion of <-1.5.

Table 7. List of differentially upregulated genes in the soleus muscle of exercised KK-A^y PAD mice.

Gene Symbol	FC	Gene Symbol	FC	Gene Symbol	FC
Tnn	47.79	*Sbk3*	2.14	*Fbln7*	1.66
Dhrs9	9.29	*Mboat2*	2.12	*Tlr2*	1.65
Chrna9	7.20	*E2f2*	2.12	*Agbl1*	1.65
Tmem8c	6.75	*Bex1*	2.10	*Map1b*	1.64

Kcnf1	5.25	*Myh4*	2.09	*Tfcp2l1*	1.64
4930539E08Rik	4.89	*Kcnk5*	2.08	*Itga9*	1.64
Igf2	4.58	*Vash2*	2.06	*Lrch1*	1.64
Neu2	4.45	*Baiap2l1*	2.04	*Soga1*	1.62
Zfp385c	4.37	*Myom2*	2.04	*Lnx2*	1.62
Slc38a1	4.25	*Malat1*	2.03	*Clcf1*	1.62
Myh8	3.97	*Ptgfr*	2.02	*Ldlrad3*	1.61
Dsp	3.75	*Mast4*	2.00	*Col20a1*	1.61
Dhx30	3.74	*Enox1*	1.96	*Igf2r*	1.60
Mtus2	3.67	*Wnt2b*	1.93	*Zc2hc1a*	1.60
Nxph4	3.59	*Klf5*	1.93	*Wee1*	1.60
Sln	3.50	*Hipk4*	1.92	*Ubash3b*	1.60
Myh3	3.42	*Fam129a*	1.92	*Strip2*	1.60
Slc6a17	3.39	*Serpinb6a*	1.90	*Cdkn1a*	1.59
Kcne1l	3.28	*Dclk1*	1.89	*Gk5*	1.59
Zdbf2	3.25	*Phlda1*	1.89	*9330151L19Rik*	1.58
3632451O06Rik	3.17	*B930095G15Rik*	1.87	*Agtrap*	1.58
Serpinb1a	2.98	*Arhgap28*	1.87	*Cx3cl1*	1.58
Mamdc2	2.92	*1110046J04Rik*	1.84	*Macf1*	1.58
2310015K22Rik	2.91	*Myoz3*	1.83	*Mtap*	1.57
Rps6ka6	2.88	*Ier3*	1.83	*Abca1*	1.57
Peg3	2.85	*Gatm*	1.83	*Tceal7*	1.57
Rrm2	2.78	*Tnfrsf23*	1.82	*Gnb3*	1.57

Ahnak2	2.74	*Pfkfb3*	1.82	*Akr1b8*	1.57
Zim1	2.72	*Kbtbd11*	1.81	*Cdc25b*	1.56
H19	2.65	*Soat1*	1.81	*Abr*	1.56
Ngef	2.59	*Slc22a17*	1.81	*Btnl9*	1.56
Piezo1	2.58	*Tmem30b*	1.80	*Dnm3os*	1.56
Peg10	2.56	*Mvd*	1.78	*Ociad2*	1.55
Map3k9	2.54	*Capn6*	1.77	*Hcn2*	1.54
Pak1	2.54	*Sbk2*	1.77	*Angptl2*	1.54
Gvin1	2.52	*Sh3rf1*	1.74	*Tubb2b*	1.54
Ucp2	2.50	*Fgd3*	1.74	*Col6a3*	1.54
Grik3	2.48	*Myl4*	1.74	*Mall*	1.54
Col7a1	2.45	*Fst*	1.73	*Sec14l5*	1.54
Lgals3	2.45	*Per1*	1.73	*Raph1*	1.54
Csnk2a1	2.43	*Hotair*	1.72	*Acer2*	1.54
Ctxn3	2.43	*Lrrc74b*	1.71	*Sacs*	1.53
Cdk6	2.42	*AI838599*	1.71	*Rfx5*	1.53
Frrs1	2.41	*Gcnt1*	1.70	*Itm2a*	1.52
Maged2	2.40	*Galnt5*	1.69	*Klrg2*	1.52
Rin1	2.30	*Zfp568*	1.69	*Fryl*	1.52
Ptpn13	2.21	*Meg3*	1.69	*Cobll1*	1.52
C77080	2.21	*Trim47*	1.69	*Tmbim1*	1.52
Vwa3a	2.21	*Slc25a24*	1.68	*Zbtb37*	1.51
Cnr1	2.18	*Galm*	1.68	*Grip2*	1.51

Zfp697	2.18	*Mamstr*	1.68	*Relb*	1.51
Arhgef37	2.18	*Calml4*	1.68	*Zfp14*	1.51
Prune2	2.18	*Trp63*	1.67	*Cpd*	1.51
Ky	2.17	*Npnt*	1.67	*Cadm1*	1.50
Eps8l2	2.15	*Nfkb2*	1.67		
Eda2r	2.14	*Adam19*	1.66		

FC, fold change.

Sedentary PAD mice (n = 4) and exercised PAD mice (n = 4). Differentially upregulated genes met an average FC criterion of >1.5.

Table 8. List of differentially downregulated genes in the soleus muscle of exercised KK-A^y PAD mice.

Gene Symbol	FC	Gene Symbol	FC	Gene Symbol	FC
Fcgbp	-68.06	*2310040G24Rik*	-1.98	*Iqcg*	-1.67
Adamts8	-5.27	*Cacna2d3*	-1.98	*Cuzd1*	-1.66
BC048679	-3.51	*Ppp1r1a*	-1.95	*Tiam1*	-1.66
Cdh22	-2.85	*Mpped2*	-1.95	*Dpyd*	-1.64
9030617O03Rik	-2.53	*Dupd1*	-1.95	*Rspo3*	-1.64
Lrtm1	-2.52	*Nt5c1a*	-1.93	*Ephx2*	-1.63
A930004D18Rik	-2.41	*Timp1*	-1.92	*Kif5c*	-1.63
Crybb1	-2.41	*Hdhd3*	-1.92	*Krt222*	-1.63
Amph	-2.37	*Kcnk2*	-1.91	*Smco1*	-1.63
Lypd6	-2.36	*C530008M17Rik*	-1.90	*Fndc5*	-1.62

Pde3b	-2.35	*Osbpl6*	-1.89	*Galt*	-1.61
Mchr1	-2.35	*Ankrd23*	-1.88	*Mylk2*	-1.61
Ankrd1	-2.31	*2310047D07Rik*	-1.84	*St3gal5*	-1.60
Dusp26	-2.27	*Fbp2*	-1.82	*Alpl*	-1.60
Slc15a5	-2.21	*Mlph*	-1.82	*Insc*	-1.60
Apobr	-2.19	*Dhcr24*	-1.81	*Fgf1*	-1.60
Dkk2	-2.18	*Dok5*	-1.81	*Lhfpl4*	-1.59
Kcng4	-2.16	*A330094K24Rik*	-1.81	*Col22a1*	-1.59
Cd209f	-2.16	*Barx2*	-1.76	*Msrb2*	-1.58
Cda	-2.15	*Dapp1*	-1.75	*Cox7a1*	-1.58
Ush1g	-2.13	*Gins2*	-1.74	*Cux2*	-1.57
Nog	-2.11	*Sv2b*	-1.72	*Lyve1*	-1.57
Tmem132d	-2.09	*Fam81a*	-1.71	*Hlf*	-1.56
Rasl10b	-2.08	*Tmem229b*	-1.71	*mt-Nd4l*	-1.56
Tbc1d1	-2.07	*Gsta4*	-1.71	*Aldh1a2*	-1.56
Gadd45b	-2.06	*Hes1*	-1.70	*Plin5*	-1.55
Cds1	-2.05	*Cytl1*	-1.69	*Rasl2-9*	-1.54
Retnla	-2.05	*Wfikkn2*	-1.69	*Tpm3*	-1.53
Masp1	-2.04	*Ccrl2*	-1.69	*Sctr*	-1.53
Kcnc4	-2.02	*Pde4a*	-1.69	*Nthl1*	-1.52
Cacna2d2	-2.01	*Plcd4*	-1.67	*Slc8a1*	-1.52
Dach2	-2.00	*Bdh1*	-1.67	*Tst*	-1.51
Pdzd3	-1.99	*Lamc3*	-1.67	*Ptgis*	-1.50

FC, fold change.

Sedentary PAD mice (n = 4) and exercised PAD mice (n = 4). Differentially downregulated genes met an average FC criterion of <-1.5.

Gene Ontology analysis was conducted for the differentially expressed genes identified between sedentary and exercised PAD mice (Tables 9 and 10). In the C57BL/6 PAD mice, extracellular matrix-related genes were ranked and downregulated (Table 9). In KK-A^y PAD mice, however, different types of genes, such as channels and transporters, were enriched (Table 10). The directions of the alteration of these enriched genes were different between the two PAD models. The direction of all the top 10 enriched GO terms was downregulation in C57BL/6 PAD mice, while the direction of most (9 of 10) of the top 10 enriched terms was upregulation in KK-A^y PAD mice.

Table 9. Enriched Gene Ontology (GO) terms for genes with altered expression induced by chronic treadmill exercise in the soleus muscle of C57BL/6 PAD mice.

Rank	Gene ontology (GO) terms	Direction	*p*-value
1	Extracellular matrix	down	1.50E-41
2	Proteinaceous extracellular matrix	down	2.20E-39
3	Collagen	down	6.90E-14
4	Ossification	down	9.20E-14
5	Cell migration	down	1.00E-12
6	Muscle contraction	down	1.20E-12
7	Urogenital system development	down	1.50E-12
8	Skeletal system development	down	2.10E-12
9	Contractile fiber	down	4.80E-12
10	Regulation of cell growth	down	5.80E-12

'down' indicates downregulation

Table 10. Enriched Gene Ontology (GO) terms for genes with altered expression induced by chronic treadmill exercise in the soleus muscle of KK-A^y PAD mice.

Rank	Gene ontology (GO) terms	Direction	*p*-value
1	Contractile fiber	up	3.20E-08
2	Proteinaceous extracellular matrix	up	2.60E-07
3	Regulation of ion transport	down	3.50E-07
4	Extracellular matrix	up	6.90E-07
5	Actin binding	up	8.80E-07
6	Cell leading edge	up	2.10E-06
7	Aging	up	2.30E-06
8	Cell growth	up	2.30E-06
9	Ion channel activity	up	2.80E-06
10	Passive transmembrane transporter activity	up	4.00E-06

'up' indicates upregulation; 'down' indicates downregulation

Discussion

In the present study, significant acute and chronic alterations were detected in the expression levels of several genes in the skeletal muscles of two different mouse models of PAD after exercise, and characterized the expression patterns of each gene. The main findings of this study are as follows: 1) exercise increased the mRNA expression of known exercise-responsive genes acutely and significantly in both C57BL/6 and KK-A^y PAD mice; 2) mRNA expression of skeletal muscle regeneration markers *Myf5* and *Myogenin* was upregulated significantly in C57BL/6 PAD mice compared to that in sham-operated mice at 3 weeks after FAL surgery, and this upregulation was inhibited significantly by exercise training; 3) *Gpr56* mRNA transcription was increased acutely and significantly by exercise in both PAD mouse models; and 4) C57BL/6 and KK-A^y PAD mice showed a different gene expression pattern in response to exercise training.

In this study, both C57BL/6 and KK-A^y PAD mice showed recovery in running performance after repeated exercise training while the hindlimb blood flow, which was significantly reduced after femoral artery ligation, was not affected by exercise training. This suggests that the running performance improvement is independent of the blood flow. Therefore, I hypothesized that the improvement of skeletal muscle function is involved in the exercise-induced recovery of running performance in PAD model mice.

Exercise induced the mRNA expressions of *Pgc1a*, *Il6*, *Nr4a1*, *Nr4a2*, and *Nr4a3* acutely in both C57BL/6 PAD and KK-A^y PAD mice. Several investigators have reported acute and chronic mRNA expression increases of *PGC1A* [72] and *NR4A* family genes [73] in exercised normal animals and healthy humans. The *PGC1* and *NR4A* families play an essential role in the control of cellular energy metabolic pathways [74, 75]; therefore, the exercise-induced upregulation of these nuclear receptors and nuclear receptor

75

coactivators is considered an important molecular mechanism underlying exercise-induced benefits through improved muscle energy metabolism [66]. IL-6 is known as a "myokine," a protein produced and secreted by skeletal muscles to fulfill paracrine or endocrine roles in insulin-sensitizing effects following exercise [76]. IL-6 is also reported to play a role in muscle hypertrophy and regeneration through the activation of muscle satellite cell functions [23, 24, 25]. The present results showing the upregulation of these important exercise-responsive genes suggest that molecular signaling to induce these genes could remain functional in the compromised skeletal muscles of animals and patients with PAD.

In C57BL/6 PAD mice, mRNA transcripts of myogenic and muscle regeneration-related *Myf5, Myogenin, Myomaker*, and *Myh3* were upregulated significantly at 3 weeks after surgery, compared to that in sham-operated mice (Table 3). This result suggested that active muscle regeneration occurred in this model. In fact, previous reports indicate the existence of regenerating myofibers, characterized by a central nucleus location, in the calf muscle of this model [26]. Treadmill exercise did not affect the expression of these myogenic and muscle regeneration-related genes acutely during the observation period (at and up to 4 h after cessation of 30-min exercise, Figure 14), whereas exercise training prevented the upregulation of *Myf5* and *Myogenin* significantly in the chronic phase (Table 3). Yang et al. investigated the time-course activation of selected myogenic (*Mrf4*, *Myf5*, *MyoD*, and *Myogenin*) genes after an acute bout of 30-min treadmill running in the calf muscle of healthy subjects [77]. Similar to the present results, they failed to detect significant differences in *Mrf4*, *Myf5*, and *Myogenin* mRNA levels at 0–24 h post-running. However they noted significant upregulation of *MyoD* mRNA levels (by 8.0-fold) at 8 h post-running. These findings suggest that the optimal selection of time points

and genes of interest are important to detect exercise-induced alterations in these myogenic and muscle regeneration-related genes. It was speculated that the exercise training-induced prevention of *Myf5* and *Myogenin* mRNA upregulation might reflect exercise-induced acceleration of the muscle regeneration process; however, detailed time-course studies of mRNA expression of the optimally-selected gene set should be performed to confirm this speculation.

The present results support the involvement of GPR56 in exercise-related molecular signaling. Rapid upregulation of *Gpr56* after the exercise session was observed in both C57BL/6 and KK-A^y PAD mice, consistent with the finding that *GPR56* expression was induced in humans by resistance exercise [70]. The mRNA expression level of *Col3a1*, an endogenous ligand of GPR56, also showed an upward trend after the treadmill exercise session. In addition, the time course of exercise-induced *Gpr56* mRNA upregulation was similar to that of *Pgc1a* in both C57BL/6 and KK-A^y PAD mice. This result agreed with the finding that *Gpr56* is a transcriptional target of PGC-1α4, a splicing variant of PGC-1α [70].

Delayed recovery of running performance was observed in the KK-A^y PAD mice compared to the C57BL/6 PAD model mice. Although there is a limitation that KK mice, the exact normal control of diabetic KK-A^y mice, was not used in this study, there should be no doubt that there is a difference in the recovery of running performance between the two because many reports have suggested that diabetic skeletal muscles have characteristics different from those of non-diabetic skeletal muscles [78–83]. In the chronic phase, the overall trend was that mRNA transcripts of myogenic and muscle regeneration-related *Myf5, Myogenin, Myomaker*, and *Myh3* were significantly upregulated or trending upward in both C57BL/6 PAD and KK-A^y PAD mice. On the

other hand, exercise training showed a different pattern: C57BL/6 PAD mice showed a significant suppression or tendency to suppress the expression of these genes, whereas KK-A^y PAD mice showed a significant upregulation or upward trend. This suggests that the skeletal muscle regeneration process in response to exercise is different in normal and diabetic mice. RNA sequence analysis followed by Gene Ontology (GO) analysis also revealed different characteristics of exercise-related alterations in the chronic phase between C57BL/6 PAD and KK-A^y PAD mice (Tables 5–10). Although there is a limitation in this study that the mechanism linking the exercise training and the gene expression data was not investigated, there are two major speculations to explain why C57BL/6 PAD and KK-A^y PAD differ in gene expression pattern. One is that because the two PAD model mice had difference in speed of running performance recovery, the two PAD model mice might have been at a different phase at the timing of skeletal muscle sampling. Detailed time-course studies of mRNA expression should be performed to confirm this speculation. Another speculation is that there was a delay in skeletal muscle regeneration in diabetic skeletal muscles, such as impaired metabolism [78], increased oxidative stress [79], chronic low-grade inflammatory profiles [80], and impaired extracellular matrix remodeling [81] and regeneration [82, 83]. Further detailed studies are needed to clarify how diabetes and the different characteristics of diabetic skeletal muscles can affect exercise-induced transcriptional alterations.

In the acute experiments, KK-A^y PAD mice showed an apparent bimodal change of *Il6* mRNA upregulation that peaked at 30 and 90 min (Figure 13B, right). However, it should be noted that the biological relevance of this bimodal change should be further confirmed, because of the relatively larger variation of the data at the 90-min time point in the present study.

In conclusion, the present study detected significant alterations in the expression of several genes in the skeletal muscles of two different mouse models of PAD upon exercise, and characterized the expression patterns of each gene. These data provide basic information about exercise-induced transcriptional alterations in the skeletal muscles in mouse PAD models which could lead to target identification for the treatment of PAD.

General Discussion

In the present study, I focused on the biology of anti-inflammatory and exercise-induced effects to clarify their physiological contribution to atherosclerotic diseases. In order to investigate the involvement of inflammation, a long-term administration study of a D5D inhibitor was performed using *ApoE* knockout mice, a murine model of atherosclerosis, and evaluated the atherosclerotic lesion area along with the inflammatory properties. In addition to this, I investigated the acute and chronic gene expression alteration caused by exercise in the soleus muscles of femoral artery-ligated mice, a murine model of PAD, in order to confirm the gene expression alteration which are known to change in exercised normal subjects, and to explore the key molecules or pathways that could mimic the benefits of exercise training under PAD conditions.

In chapter 1, I demonstrated that a D5D inhibitor, compound-326, exerts anti-atherosclerotic effects in *ApoE* knockout mice with two different protocols for atherosclerosis development. Compound-326 reduced the atherosclerotic lesion area in a dose-dependent manner with similar effective dose ranges in the two protocols with different states of inflammation [21, 37]. In both protocols, the anti-atherosclerotic effect was accompanied by decreased hepatic arachidonic acid levels and increased hepatic DGLA levels; consequently decreasing the blood production of pro-inflammatory arachidonic acid-derived eicosanoids and increased blood production of an anti-inflammatory DGLA-derived eicosanoid. Compound-326 reduced plasma sICAM-1 levels without altering the plasma cholesterol levels in both protocols, which further supports that anti-inflammatory effects are the main mechanism of atherosclerotic effects caused by D5D inhibition [57–60]. These results clearly indicate the involvement of D5D and its role in vascular inflammation in atherogenesis, which provide significant insight to the anti-inflammatory strategy as well as the application of D5D-related biology to the

treatment of atherosclerosis [4].

In chapter 2, significant acute and chronic alterations were detected in the expression levels of several genes in the skeletal muscles of two different mouse models of PAD after exercise. It was confirmed that both normal C57BL/6 and diabetic KK-A^y PAD model mice can improve running performance by repeated treadmill exercise training while the hindlimb blood flow, which was significantly reduced after the femoral artery ligation, was not affected by the exercise training. This indicates that the running performance improvement was independent of the blood flow recovery and thus was hypothesized that improvement in skeletal muscle function was involved [66, 74, 75]. To demonstrate this, acute mRNA expression increase of known exercise-responsive genes was confirmed in both PAD models. Furthermore, mRNA expression of skeletal muscle regeneration markers *Myf5* and *Myogenin* was significantly upregulated in C57BL/6 PAD mice, and this upregulation was significantly inhibited by exercise training [77]. KK-A^y PAD mice showed a different pattern; these mRNA expressions just showed upward trends and tended to further upregulate by exercise training. RNA sequence analysis was performed to identify the differentially expressed genes between sedentary and exercised PAD mice. Interestingly, of the 37 genes overlapped between C57BL/6 PAD mice and KK-A^y PAD mice among the differentially expressed genes, upregulated or downregulated after exercise, 31 genes were downregulated in C57BL/6 PAD mice, but upregulated in KK-A^y PAD mice, showing a negative correlation. Gene Ontology analysis conducted for the differentially expressed genes identified revealed that types of genes regulated and the directions of the alteration were different between the two PAD model mice; extracellular matrix-related genes were ranked and downregulated in C57BL/6 PAD mice, genes related to channels and transporters were enriched, mostly upregulated, in KK-A^y PAD

mice [78–83]. To the best of my knowledge, this is the first study to obtain basic information about exercise-induced transcriptional alterations in the skeletal muscles in mouse PAD models, providing significant findings to identify the key molecules or pathways that could mimic the benefits of exercise training under PAD conditions.

In conclusion, these results provide novel evidence for the involvement of vascular inflammation suppression and of skeletal muscle function improvement in the treatment of atherosclerosis. The present results also indicate the clear engagement of D5D in the development of atherosclerosis. These are not only of great academic significance in the fields of vascular inflammation and skeletal muscle function, but also open the way for the development of new therapeutic agents and other strategies for the treatment of atherosclerotic diseases.

Acknowledgements

References

1. World Health Organization. The top 10 causes of death (2020).

    https://www.who.int/news-room/fact-sheets/detail/the-top-10-causes-of-death

2. Fuster V. Global burden of cardiovascular disease: time to implement feasible

    strategies and to monitor results. J Am Coll Cardiol. 2014;64(5):520-2.

3. Mackay J, Mensah G. Atlas of heart disease and stroke. World Health Organization;

    2004:84–91.

4. Roger VL, Go AS, Lloyd-Jones DM, et al. Heart disease and stroke statistics--2012

    update: A report from the American Heart Association. Circulation.

    2012;125(1):e12–e220.

5. Libby P. Inflammation in atherosclerosis. Nature. 2002;420(6917):868–874.

6. Criqui MH, Aboyans V. Epidemiology of peripheral artery disease. Circ Res.

    2015;116:1509-1526.

7. Fowkes FG, Rudan D, Rudan I, Aboyans V, Denenberg JO, McDermott MM, et al.

    Comparison of global estimates of prevalence and risk factors for peripheral artery

    disease in 2000 and 2010: a systematic review and analysis. Lancet. 2013;382:1329-

    1340.

8. Hiatt WR, Armstrong EJ, Larson CJ, Brass EP. Pathogenesis of the limb

    manifestations and exercise limitations in peripheral artery disease. Circ Res.

    2015;116: 1527-1539.

9. Fokkenrood HJ, Bendermacher BL, Lauret GJ, Willigendael EM, Prins MH, Teijink

    JA. Supervised exercise therapy versus non-supervised exercise therapy for

    intermittent claudication. Cochrane Database Syst Rev. 2013;8: CD005263.

10. Geovanini GR, Libby P. Atherosclerosis and inflammation: overview and updates.

    Clin Sci (Lond). 2018;132(12):1243-1252.

11. Firnhaber JM, Powell CS. Lower Extremity Peripheral Artery Disease: Diagnosis and Treatment. Am Fam Physician. 2019;99(6):362-369.

12. Murphy TP, Cutlip DE, Regensteiner JG, Mohler ER, Cohen DJ, Reynolds MR, et al. Supervised exercise versus primary stenting for claudication resulting from aortoiliac peripheral artery disease: six-month outcomes from the claudication: exercise versus endoluminal revascularization (CLEVER) study. Circulation. 2012;125: 130-139.

13. Stewart KJ, Hiatt WR, Regensteiner JG, Hirsch AT. Exercise training for claudication. N Engl J Med. 2002;347: 1941-1951.

14. Hiatt WR, Regensteiner JG, Wolfel EE, Carry MR, Brass EP. Effect of exercise training on skeletal muscle histology and metabolism in peripheral arterial disease. J Appl Physiol (1985). 1996;81:780-788.

15. Hiatt WR, Wolfel EE, Meier RH, Regensteiner JG. Superiority of treadmill walking exercise versus strength training for patients with peripheral arterial disease. Implications for the mechanism of the training response. Circulation. 1994;90: 1866-1874.

16. Ridker PM, Everett BM, Thuren T, et al. Antiinflammatory Therapy with Canakinumab for Atherosclerotic Disease. N Engl J Med. 2017;377(12):1119-1131.

17. Ridker PM, Devalaraja M, Baeres FMM, Engelmann MDM, Hovingh GK, Ivkovic M, et al. IL-6 inhibition with ziltivekimab in patients at high atherosclerotic risk (RESCUE): a double-blind, randomised, placebo-controlled, phase 2 trial. Lancet 2021;397(10289):2060-2069.

18. Charo IF, Taub R. Anti-inflammatory therapeutics for the treatment of atherosclerosis. Nat Rev Drug Discov. 2011;10(5):365–376.

19. Libby P, Aikawa M. Stabilization of atherosclerotic plaques: new mechanisms and clinical targets. Nat Med. 2002;8(11):1257–1262.

20. Powell DR, Gay JP, Smith M, et al. Fatty acid desaturase 1 knockout mice are lean with improved glycemic control and decreased development of atheromatous plaque. Diabetes Metab Syndr Obes. 2016;9:185–199.

21. Takagahara S, Shinohara H, Itokawa S, et al. A Novel Orally Available Delta-5 Desaturase Inhibitor Prevents Atherosclerotic Lesions Accompanied by Changes in Fatty Acid Composition and Eicosanoid Production in ApoE Knockout Mice. J Pharmacol Exp Ther. 2019;371(2):290–298.

22. Pedersen BK, Febbraio MA. Muscle as an endocrine organ: focus on muscle-derived interleukin-6. Physiol Rev. 2008;88:1379-1406.

23. Serrano AL, Baeza-Raja B, Perdiguero E, Jardí M, Muñoz-Cánoves P. Interleukin-6 is an essential regulator of satellite cell-mediated skeletal muscle hypertrophy. Cell Metab. 2008;7:33-44.

24. Toth KG, McKay BR, De Lisio M, Little JP, Tarnopolsky MA, Parise G. IL-6 induced STAT3 signalling is associated with the proliferation of human muscle satellite cells following acute muscle damage. PLoS One. 2011;6: e17392.

25. Muñoz-Cánoves P, Scheele C, Pedersen BK, Serrano AL. Interleukin-6 myokine signaling in skeletal muscle: a double-edged sword? FEBS J. 2013;280: 4131-4148.

26. Sugo T, Terada M, Oikawa T, Miyata K, Nishimura S, Kenjo E, *et al.* Development of antibody-siRNA conjugate targeted to cardiac and skeletal muscles. J Control Release. 2016;237: 1-13.

27. Mahoney DJ, Parise G, Melov S, Safdar A, Tarnopolsky MA. Analysis of global mRNA expression in human skeletal muscle during recovery from endurance exercise. FASEB J. 2005;19: 1498-1500.

28. Yang Y, Creer A, Jemiolo B, Trappe S. Time course of myogenic and metabolic gene expression in response to acute exercise in human skeletal muscle. J Appl Physiol (1985). 2005;98(5):1745-52.

29. Cho HP, Nakamura M, Clarke SD. Cloning, expression, and fatty acid regulation of the human delta-5 desaturase. J Biol Chem. 1999;274(52):37335–37339.

30. Matsuzaka T, Shimano H, Yahagi N, et al. Dual regulation of Δ^5- and Δ^6-desaturase gene expression by SREBP-1 and PPARα. J Lipid Res. 2002;43(1):107–114.

31. Leonard AE, Kelder B, Bobik EG, et al. cDNA cloning and characterization of human Delta5-desaturase involved in the biosynthesis of arachidonic acid. Biochem J. 2000;347:719–724.

32. De Caterina R, Zampolli A. From asthma to atherosclerosis- 5-lipoxygenase, leukotrienes, and inflammation. N Engl J Med. 2004:350(1):4–7.

33. Kwak JH, Paik JK, Kim OY, et al. FADS gene polymorphisms in Koreans: association with ω6 polyunsaturated acids in serum phospholipids, lipid peroxides, and coronary artery disease. Atherosclerosis. 2011;214(1):94–100.

34. Martinelli N, Girelli D, Malerba G, et al. FADS genotypes and desaturase activity estimated by the ratio of arachidonic acid to linoleic acid are associated with inflammation and coronary artery disease. Am J Clin Nutr. 2008;88(4):941–949.

35. Yashiro H, Takagahara S, Tamura YO, et al. A novel selective inhibitor of delta-5 desaturase lowers insulin resistance and reduces body weight in diet-induced obese C57BL/6J mice. PLoS One. 2016;11(11):e0166198.

36. Getz GS, Reardon CA. Diet and murine atherosclerosis. Arterioscler Thromb Vasc Biol. 2006;26(2):242–249.

37. Nakashima Y, Plump AS, Raines EW, et al. ApoE-deficient mice develop lesions of all phases of atherosclerosis throughout the arterial tree. Arterioscler Thromb. 1994;14(1):133–140.

38. Paigen B. Genetics of responsiveness to high-fat and high-cholesterol diets in the mouse. Am J Clin Nutr. 1995;62(2):458S–462S.

39. Jawien J, Nastalek P, Korbut R. Mouse models of experimental atherosclerosis. J Physiol Pharmacol. 2004;55(3):503–517.

40. Veillard NR, Steffens S, Burger F, et al. Differential expression patterns of proinflammatory and antiinflammatory mediators during atherogenesis in mice. Arterioscler Thromb Vasc Biol. 2004;24(12):2339–2344.

41. Lusis AJ. Atherosclerosis. Nature. 2000;407(6801):233–241.

42. Ross R. Atherosclerosis--an inflammatory disease. N Engl J Med. 1999;340(2):115–126.

43. Libby P, Ridker PM, Maseri A. Inflammation and atherosclerosis. Circulation. 2002;105(9):1135–1143.

44. Puntmann VO, Bigalke B, Nagel E. Characterization of the inflammatory phenotype in atherosclerosis may contribute to the development of new therapeutic and preventative interventions. Trends Cardiovasc Med. 2010;20(5):176–181.

45. Agren JJ, Julkunen A, Penttila I. Rapid separation of serum lipids for fatty acid analysis by a single aminopropyl column. J Lipid Res. 1992;33(12):1871–1876.

46. Babaev VR, Chew JD, Ding L, et al. Macrophage EP4 deficiency increases apoptosis and suppresses early atherosclerosis. Cell Metab. 2008;8(6):492–501.

47. Kobayashi T, Tahara Y, Matsumoto M, et al. Roles of thromboxane A (2) and prostacyclin in the development of atherosclerosis in apoE-deficient mice. J Clin Invest. 2004;114(6):784–794.

48. Heller EA, Liu E, Tager AM, et al. Inhibition of atherogenesis in BLT1-deficient mice reveals a role for LTB4 and BLT1 in smooth muscle cell recruitment. Circulation. 2005;112(4):578–586.

49. Subbarao K, Jala VR, Mathis S, et al. Role of leukotriene B4 receptors in the development of atherosclerosis: potential mechanisms. Arterioscler Thromb Vasc Biol. 2004;24(2):369–375.

50. Ziboh VA, Miller CC, Cho Y. Metabolism of polyunsaturated fatty acids by skin epidermal enzymes: generation of antiinflammatory and antiproliferative metabolites. Am J Clin Nutr. 2000;71(1 Suppl):361S–366S.

51. Takai S, Jin D, Kawashima H, et al. Anti-atherosclerotic effects of dihomo-γ-linolenic acid in ApoE-deficient mice. J Atheroscler Thromb. 2009;16(4):480–489.

52. Palumbo B, Oguogho A, Fitscha P, et al. Prostaglandin E1-therapy reduces circulating adhesion molecules (ICAM-1, E-selectin, VCAM-1) in peripheral vascular disease. Vasa. 2000;29:179–185.

53. Takahashi HK, Iwagaki H, Tamura R, et al. Unique regulation profile of prostaglandin E1 on adhesion molecule expression and cytokine production in human peripheral blood mononuclear cells. J Pharmacol Exp Ther. 2003;307(3):1188–1195.

54. Wang X, Lin Y, Luo N, et al. Short-term intensive atorvastatin therapy improves endothelial function partly via attenuating perivascular adipose tissue inflammation

through 5-lipoxygenase pathway in hyperlipidemic rabbits. Chin Med J (Engl). 2014;127(16):2953-9.

55. Darrow AL, Shohet RV, Maresh JG. Transcriptional analysis of the endothelial response to diabetes reveals a role for galectin-3. Physiol Genomics. 2011;43(20):1144-52.

56. Martínez-Clemente M, Ferré N, González-Périz A, et al. 5-lipoxygenase deficiency reduces hepatic inflammation and tumor necrosis factor alpha-induced hepatocyte damage in hyperlipidemia-prone ApoE-null mice. Hepatology. 2010;51(3):817-27.

57. Witkowska AM. Soluble ICAM-1: a marker of vascular inflammation and lifestyle. Cytokine. 2005;31(2):127–134.

58. Nguyen QM, Srinivasan SR, Xu JH, et al. Distribution and cardiovascular risk correlates of plasma soluble intercellular adhesion molecule-1 levels in asymptomatic young adults from a biracial community: the Bogalusa Heart Study. Ann Epidemiol. 2010;20(1):53–59.

59. Marcinkowski M, Czarnecka D, Jastrzebski M, et al. Inflammatory markers 10 weeks after myocardial infarction predict future cardiovascular events. Cardiol J. 2007;14(1):50–58.

60. Rallidis LS, Zolindaki MG, Vikelis M, et al. Elevated soluble intercellular adhesion molecule-1 levels are associated with poor short-term prognosis in middle-aged patients with acute ischaemic stroke. Int J Cardiol. 2009;132(2):216–220.

61. Aiello RJ, Bourassa PA, Lindsey S, et al. Monocyte chemoattractant protein-1 accelerates atherosclerosis in apolipoprotein E-deficient mice. Arterioscler Thromb Vasc Biol. 1999;19(6):1518–1525.

62. Ni W, Egashira K, Kitamoto S, et al. New anti-monocyte chemoattractant protein-1 gene therapy attenuates atherosclerosis in apolipoprotein E-knockout mice. Circulation. 2001;103(16):2096–2101.

63. Khodabandehloo H, Gorgani-Firuzjaee S, Panahi G, et al. Molecular and cellular mechanisms linking inflammation to insulin resistance and β-cell dysfunction. Transl Res. 2016;167(1):228–256.

64. Welty FK, Alfaddagh A, Elajami TK. Targeting inflammation in metabolic syndrome. Transl Res. 2016;167(1):257–280.

65. Moon YA, Hammer RE, Horton JD. Deletion of ELOVL5 leads to fatty liver through activation of SREBP-1c in mice. J Lipid Res. 2009;50(3):412–423.

66. Zhao Y, Bruemmer D. NR4A orphan nuclear receptors: transcriptional regulators of gene expression in metabolism and vascular biology. Arterioscler Thromb Vasc Biol. 2010;30: 1535-1541.

67. Lotfi S, Patel AS, Mattock K, Egginton S, Smith A, Modarai B. Towards a more relevant hind limb model of muscle ischaemia. Atherosclerosis. 2013;227: 1-8.

68. Belch J, MacCuish A, Campbell I, Cobbe S, Taylor R, Prescott R, et al. The prevention of progression of arterial disease and diabetes (POPADAD) trial: factorial randomised placebo controlled trial of aspirin and antioxidants in patients with diabetes and asymptomatic peripheral arterial disease. BMJ. 2008;337: a1840.

69. He S, Zhao T, Guo H, Meng Y, Qin G, Goukassian DA, et al. Coordinated Activation of VEGF/VEGFR-2 and PPARδ Pathways by a Multi-Component Chinese Medicine DHI Accelerated Recovery from Peripheral Arterial Disease in Type 2 Diabetic Mice. PLoS One. 2016;11: e0167305.

70. Morimoto Y, Bando YK, Shigeta T, Monji A, Murohara T. Atorvastatin prevents ischemic limb loss in type 2 diabetes: role of p53. J Atheroscler Thromb. 2011;18: 200-208.

71. White JP, Wrann CD, Rao RR, Nair SK, Jedrychowski MP, You JS, et al. G protein-coupled receptor 56 regulates mechanical overload-induced muscle hypertrophy. Proc Natl Acad Sci U S A. 2014;111: 15756-15761.

72. Norheim F, Langleite TM, Hjorth M, Holen T, Kielland A, Stadheim HK, et al. The effects of acute and chronic exercise on PGC-1α, irisin and browning of subcutaneous adipose tissue in humans. FEBS J. 2014;281: 739-749.

73. Catoire M, Mensink M, Boekschoten MV, Hangelbroek R, Müller M, Schrauwen P, et al. Pronounced effects of acute endurance exercise on gene expression in resting and exercising human skeletal muscle. PLoS One. 2012;7: e51066.

74. Finck BN, Kelly DP. PGC-1 coactivators: inducible regulators of energy metabolism in health and disease. J Clin Invest. 2006;116: 615-622.

75. Pearen MA, Muscat GE. Minireview: Nuclear hormone receptor 4A signaling: implications for metabolic disease. Mol Endocrinol. 2010;24: 1891-1903.

76. Pal M, Febbraio MA, Whitham M. From cytokine to myokine: the emerging role of interleukin-6 in metabolic regulation. Immunol Cell Biol. 2014;92: 331-339.

77. Yang Y, Creer A, Jemiolo B, Trappe S. Time course of myogenic and metabolic gene expression in response to acute exercise in human skeletal muscle. J Appl Physiol (1985). 2005;98(5): 1745-1752.

78. Bianchi L, Volpato S. Muscle dysfunction in type 2 diabetes: a major threat to patient's mobility and independence. Acta Diabetol. 2016;53: 879-889.

79. Aragno M, Mastrocola R, Catalano MG, Brignardello E, Danni O, Boccuzzi G. Oxidative stress impairs skeletal muscle repair in diabetic rats. Diabetes. 2004;53: 1082-1088.

80. McKay BR, Ogborn DI, Baker JM, Toth KG, Tarnopolsky MA, Parise G. Elevated SOCS3 and altered IL-6 signaling is associated with age-related human muscle stem cell dysfunction. Am J Physiol Cell Physiol. 2013;304: C717-C728.

81. Gopinath SD, Rando TA. Stem cell review series: aging of the skeletal muscle stem cell niche. Aging Cell. 2008;7: 590-598.

82. Sala D, Zorzano A. Differential control of muscle mass in type 1 and type 2 diabetes mellitus. Cell Mol Life Sci. 2015;72: 3803-3817.

83. D'Souza DM, Al-Sajee D, Hawke TJ. Diabetic myopathy: impact of diabetes mellitus on skeletal muscle progenitor cells. Front Physiol. 2013;4: 379.